A MODEL REVIEW AND PROPOSED MECHANISTIC TILLER MODEL FOR THE CANEGRO SUGARCANE CROP MODEL

by

Carel Nicolaas Bezuidenhout

Dissertation submitted in the compliance with the requirements for the Masters Degree in Technology: Electronic Engineering, Light Current, in the Faculty of Engineering at Technikon Natal, Durban.

March 2000

This dissertation represents my own work in both conception and execution

C.N. Bezuidenhout

APPROVED FOR FINAL SUBMISSION

Supervisor: Professor Vladimir B. Bajic, Pr. Eng., D. Eng. Sc.(E.E.)

Joint supervisor: Doctor Garry J. O'Leary, B.Agr.Sc.(Hons), M.Agr.Sc., Ph.D.

April 05, 2000

Date

Acknowledgements

The author would like to thank his supervisors, Prof. V.B. Bajic from Technikon Natal and Dr. G.J. O'Leary from the South African Sugar Association for their devotion and guidance shown during the course of this study. Suggestions and guidance from Dr. A. Singels from the South African Sugar Association Experiment Station is also greatly appreciated. Acknowledgements for valuable input go to the following persons at the South African Sugar Association Experiment Station: Mr. R.A. Donaldson, Dr. R. v. Antwerpen, Mr. M. Murdoch and Mr. E. Schmidt. Discussions with Mr. M. McGlinchey from the Swazi Sugar Association Extension Services and Dr. N.G. Inman-Bamber from the CSIRO, Townsville, Australia, also provided valuable information regarding the CANEGRO model's current content. Dr. N.G. Inman-Bamber, Dr. A. Singels, Mr. M. Murdoch, Mr. M. McGlinchey, Mr. J.A. Kennedy, Mr. S. Kanniapen and Mr. M. Akbar Khan were involved in designing, managing and recording the field experiment of which the results were used in this study. Mrs. C. Brown and Mrs. B. Bezuidenhout assisted with proof reading and editing.

The South African Sugar Association Experiment Station is thanked for providing funding and granting study leave for this study. This institute also facilitated experimental trials, equipment and a reference library.

Abstract

The CANEGRO model is a mechanistic model that describes environmental, physiological and managerial features of the agricultural sugarcane production system. The model originated from many sources of crop, climatic and soil research work. This caused a fragmentation in the model's components. The objectives of this study was to give a detailed model overview after an investigation into the model's code, published and unpublished documentation and to propose a mechanistic approach in the modelling of tiller populations. The sugarcane production system was described according to its driving factors, which were subdivided into those of the environment and those of the plant. Environmental influences were subdivided into the atmosphere and the soil, while the plant could be subdivided into crop and tiller phenology, photosynthesis and carbon utilisation, the root system and water related stress reaction. The second part of this study aimed at developing a mechanistic tiller population model. The following five tiller population phases were identified: pre-germination, pre-emergence, primary tiller emergence, secondary tiller emergence and tiller senescence. Pre-germination, pre-emergence and primary tiller emergence were the first three phases and were assumed to be driven by the initial number of buds in the soil and accumulated thermal time. The fourth phase, secondary tiller development, was assumed to be driven by thermal time and canopy cover while the fifth phase, tiller senescence, was assumed to be driven by the ability of individual tillers to compete for limited light resources. Tiller age was used to determine total leaf number per tiller and leaf area per tiller, which were used to derive the crop's leaf area index and light interception. Experimental data was used to calibrate the model. The new model was validated and outperformed the current CANEGRO model. The mechanistic nature of the new model should allow for a better understanding of the effect of light competition and different agronomic practices on sugarcane growth and was the first of its kind to be proposed for the CANEGRO model.

Table of contents

Summary of tables

Summary of figures

Abbreviations and definitions of terms

ASCE	American Society of Civil Engineers.
Biomass	The remaining mass of plant material after all water was removed.
Bud	A miniature stem with its growing point, primordia of leaves and roots. A bud forms a new shoot when germination is entered.
Crop	A collection of sugarcane plants that develop together are exposed to similar agronomic conditions.
CSSA	Crop Science Society of America.
DSSAT	A Decision Support System for Agrotechnology Transfer.
Evapotranspiration	The atmosphere's potential evaporative demand from the soil, water surfaces and plants.
LAI	Leaf area index, which is the total green leaf area per unit land surface
Light interception	The fraction of PAR that was intercepted by the crop
PAR	Photosynthetically-active radiation, falling in a waveband of 400-700*nm*.
Phenology	The description of distinct sequential morphological phases of a plant.
Phyllochron interval	A temperature related time laps between the emergence of sequential leaves on a plant.
Population	Plant density on a standard surface area.
Ratoon	Oppose to a planted crop, a ratoon crop emerges from the remains of a harvested existing crop.
Row spacing	Distance between consecutive furrows in which sugarcane was planted.
Runoff	Above surface water that is unable to infiltrate the soil.
Secondary tiller	A tiller that emerged from a parent, which is actively growing and sharing photosynthate.
SCS	U.S. Soil Conversion Service.

Shoot	A germinated bud that has not yet developed its own leaves to become a sustainable tiller.
Stool	The collective number of tillers that originate from a single planted bud.
Telomechron interval	The temperature related interval between the emergence of a tiller and the emergence of its first secondary tiller.
Tiller	The smallest self-sustainable unit in a sugarcane crop. Consists of a stalk, leaves and roots. Roots could be shared with other tillers.
Tillering	The process involved for a tiller to reproduce secondary tillers.

Chapter 1

INTRODUCTION

1.1. Background to this study

Sugarcane (*Saccharum* species hybrids) is a tall and upright member of the grass family. It is a tropical plant and grows well under tropical and sub-tropical conditions with high amounts of water and radiation. Mature sugarcane has significantly high levels of sucrose stored in the parenchyma tissue in the stalk. This makes sugarcane a commercially viable agricultural crop. Sugarcane production has been extended to hot arid areas where it is irrigated. Various countries practice sugarcane farming under many different climatic and management conditions.

Sugarcane is farmed under variable agronomic and climatic conditions in South Africa. Different cultivars (also called varieties) interact differently to external factors like crop age, season and pests (e.g. Inman-Bamber, 1985).

The sugarcane production system is defined by relationships between influencing factors of the environment and the plant, or crop as a whole. This system is complex and evolving. Environmentally, factors can be subdivided into atmospheric and soil conditions. These factors drive many of the processes that take place within the plant. Managerial decisions are often made to exploit the plant to maximise an economic harvest. These may include adjustments to soil properties like nitrogen (e.g. Meyer and Wood, 1994) or water (e.g. Thompson, 1976; McGlinchey *et al.*, 1995) or adjustments to the atmosphere by means of controlling the planting season (Inman-Bamber, 1994a). Other managerial adjustments, like row spacing (e.g. Kanwar and Sharma, 1974), herbicide and pest control (e.g. Leslie, 1997) and drying off (e.g. Robertson and Donaldson, 1998) optimise integrated relationships

between the plant and its environment to maximise profits. Figure 1.1 illustrates some typical factors that are considered to play important roles in the sugarcane system.

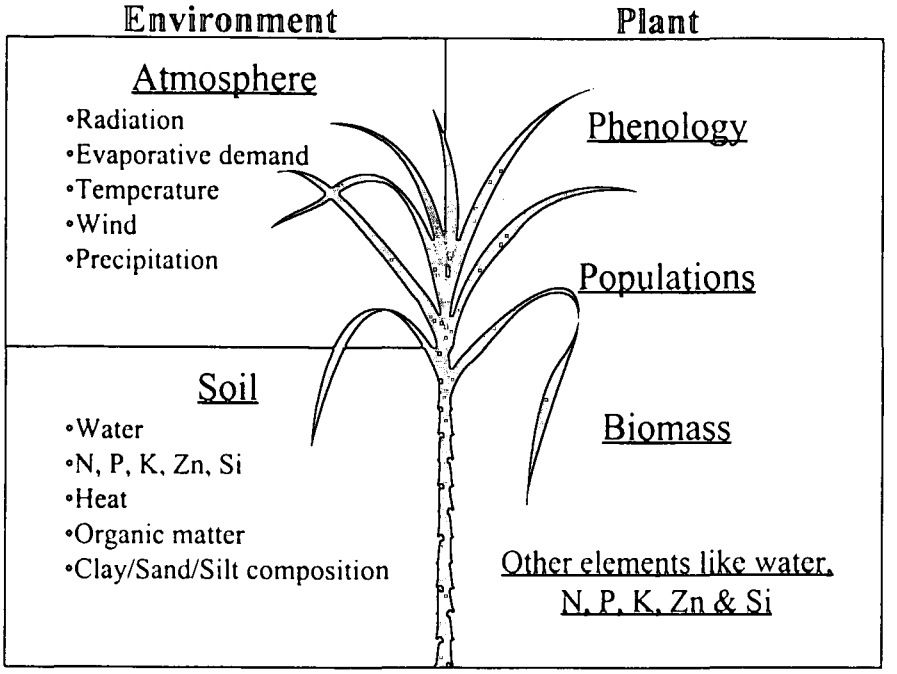

Figure 1.1. An overview of the sugarcane production system and its environmental driving factors.

1.2. Modelling the sugarcane production system

Various components of the sugarcane production system have been implemented in a simulation model, named CANEGRO. This generally mechanistic model describes some environmental, physiological and managerial features of the agricultural sugarcane production system. The CANEGRO model is the most comprehensive sugarcane model calibrated and validated under South African conditions (Inman-Bamber, 1995b). It has been included as the sugarcane model for *A Decision Support System for Agrotechnology Transfer* (DSSAT) by the *International Benchmark Sites Network for Agrotechnology Transfer* (IBSNAT) and is used in various other sugarcane production regions in the world. Because of the complexity of the sugarcane production system, the CANEGRO model is not static and future refinements are anticipated.

The model is based on research from many crop, climatic and soil aspects. Some work was conducted on different crops and was later adapted for sugarcane. Other work was specifically conducted on sugarcane and often included different sugarcane cultivars and managerial scenarios. Because of the complexity of the system, experiments were designed to concentrate on certain aspects of the system. Individual experiments could therefore only give limited explanations of the system and in order to obtain a more comprehensive mechanistic model, results from many experiments were finally integrated through a computer programme.

The continuous model building process makes model documentation difficult. Scientific papers and reviews, reporting on specific components of the model, have been published over a number of years. Inman-Bamber and Kiker published the computer code in the DSSAT system in 1997.

With regard to the above mentioned scant documentation, the need emerged to undertake a comprehensive model review in order to (1) document and refine the model and (2) develop a structure to facilitate future anticipated adjustments and additions. The aim of this study was to initiate this review by selecting appropriate components for review and examination.

This study had two main objectives:

1. To give a detailed model overview after interpreting the model code and surveying all published and unpublished work with respect to the model. A specific objective was to identify areas where refinements to existing model components could be anticipated. This excluded the description of larger model sections. For example a nitrogen balance is the subject of another study.
2. To integrate a limited number of fragmented existing model components and to introduce mechanistic driving factors. The specific objective was to integrate the properties that describe the crop's tiller population and foliage by reviewing differential equations and

applying statistical methods to represent variability. This included a re-analysis of previously collected experimental data.

Chapters 2 and 3 describe the existing CANEGRO model and chapter 4 reviews some fragmented crop properties, proposing a more mechanistic tiller model.

Chapter 2

THE ENVIRONMENTAL ASPECTS OF THE CANEGRO SUGARCANE MODEL

2.1. Atmospheric Properties

Daily meteorological observations define the atmosphere in the CANEGRO model. These observations are made in a standardised way over many years at various sites within the sugar producing areas (*e.g.* Singels and Bezuidenhout, 1999). A daily observation will typically include minimum and maximum temperature (°*C*), precipitation (*mm*), wind run ($km \times d^{-1}$), class A-pan evaporation (*mm*), wet and dry bulb temperatures at 8:00 and 14:00 (°*C*) and sunshine duration (*h*). From these observations, various other atmospheric properties can be derived by making use of standardised equations.

2.1.1. Temperature

Temperature is regarded as one of the main driving forces to some physiological and physical processes in the sugarcane plant and its environment. Minimum and maximum temperatures are easily measured on a daily basis. Temperature and rainfall are the most widespread recorded atmospheric conditions (Smith, 1992:7) and are therefore important for the testing and extrapolation of models. Inman-Bamber (1995b) indicated that climatic constraints for sugarcane performance varying over latitude and altitude, are temperature dependant. Correlations between temperature, sugarcane leaf properties and stalk populations were identified and described by Inman-Bamber (1991). Temperature also affects respiration (Glover, 1972) and the saturation point of vapour in the air (Wang, 1967: 37), which affects soil evaporation and plant transpiration (ASCE 1990, 145-160; Allen *et al.*, 1989). Way (1995) indicated various responses between developmental stages of a common South African

stalk borer *Eldana saccharina* (Lepidoptera: Pyralidae) and temperature. Coleman (1968) also noted the important role temperature plays in the flowering process of sugarcane.

Daily heat units (HU_B in $°C \times d$), also known as thermal time, is a common temperature property that is used in biological modelling.

$$HU_B = \max\{0,\ \overline{T} - B\} \tag{2.1.1}$$

where $\overline{T}$ ($°C$) respresents the average temperature for the day and B ($°C$) is a process determined base temperature.

Inman-Bamber (1994b) calculated $\overline{T}$ with:

$$\overline{T} = \frac{T_{Min} + T_{Max}}{2} \tag{2.1.2}$$

where T_{Min} and T_{Max} ($°C$) are the measured minimum and maximum temperatures for the day.

The base temperature (B) denotes the sensitivity of physiological processes to temperature. Leaf emergence and various other growth processes have been successfully simulated with HU_{10} (Inmam-Bamber, 1994b; Van Antwerpen, 1998: 48), while HU_{16} was used for tiller population calculations (Inman-Bamber and Kiker, 1997).

An accumulating effect of temperature can be expressed by accumulating HU_B over days. This is denoted as ΣHU_B and is expressed in $°C \times d$.

2.1.2. Solar radiation

Van Dillewijn (1952: 120) noted that solar radiation is one of the most influential factors in sugarcane production. Studies by Inman-Bamber (1995b) investigated limitations of sugarcane production to solar radiation in the Southern African context. Solar radiation plays an active role in photosynthesis (Thornley, 1976: 111-122; Spitters *et al.*, 1986) and in

evapotranspiration (ASCE, 1990: 100-103). In the CANEGRO model solar radiation is expressed in $MJ \times m^{-2} \times d^{-1}$. If $cal \times cm^{-2} \times d^{-1}$ was measured, the value is converted as follows (Servay, 1986: 438):

$$10^{-4} cal \times cm^{-2} \times d^{-1} = 4.186 J \times m^{-2} \times d^{-1} \quad (2.1.3)$$

If solar radiation was not directly measured a value is derived from sunshine duration and extraterrestrial radiation. Spitters *et al.* (1986) calculated daily extraterrestrial radiation (S_{er} in $J \times m^{-2} \times d^{-1}$) as follows:

$$S_{er} = \int S'_{sc} \sin \beta \; dt_h \quad (2.1.4)$$

where (S'_{sc} in $J \times m^{-2} \times s^{-1}$) is the extraterrestrial flux, β is the angle of the sun above the horizon and t_h is time (solar hour).

Clear sky surface radiation (S_{csr} in $MJ \times m^{-2} \times d^{-1}$) was noted by the ASCE (1990: 134) to be 75% of extraterrestrial radiation.

$$S_{csr} = 0.75 S_{er} \times 10^{-6} \quad (2.1.5)$$

Thompson (1986: 26-27) used an empirically calibrated function to derive actual daily solar radiation (S_{ac} in $MJ \times m^{-2} \times d^{-1}$).

$$S_{ac} = S_{er} \left(0.29 \cos \phi + 0.52 \left(\frac{d}{D}\right)\right) \times 10^{-6} \quad (2.1.6)$$

where D is the daylength in hours from sunrise to sunset (Spitters *et al.*, 1986), d is the measured number of sunshine hours for the day (Lambrecht Instruments, Göttingen, Germany) and ϕ is the latitude.

The coefficient for determining the influence of cloud cover, 0.52 (eq 2.1.6), was callibrated for Pongola (*27°24' S, 31°35' E, elev. 308m*). Although currently constant, this coefficient

tends to be climatically dependant (*pers. comm. M. McGlinchey, Swazi Sugar Association Extension Services, Simunye*, 1999).

Photosynthetically-active radiation (*PAR* in $MJ \times m^{-2} \times d^{-1}$), falling in a waveband of 400-700*nm* (Spitters *et al.*, 1986), was assumed to be consistently 50% of S_{ac} (Inman-Bamber, 1991). A scattered diffuse component in *PAR* that changes in wavelength distribution under overcast conditions (Spitters *et al.*, 1986) was not included.

2.1.3. Evapotranspiration

On a vegetative field the evaporative demand for the field will unavoidably include vapour diffusion through plant stomata, also known as transpiration (Wang, 1967: 140; Allen *et al.*, 1989). Evapotranspiration, expressed in $mm^3 \times mm^{-2} \times d^{-1}$ or simply *mm* per day thereby describes the combined effect of evaporation from soil, water surfaces and plants. Thompson (1976) found a direct relationship between the accumulated biomass of sugarcane and the total amount of evapotranspiration since the beginning of a crop. He concluded that approximately 9.7*t* sugarcane per hectare (equivalent to about 1.35*t* sucrose per hectare) could be produced with every 100*mm* of water evapotranspiration. This is locally known as the Thompson model.

An unlimited supply of water will bring evapotranspiration to its full capacity, this is known as potential evapotranspiration (E_T) (Wang, 1967: 140), atmospheric evaporative demand (de Jager and van Zyl, 1989) or reference cane evaporation (Singels *et al.*, 1998). Under normal farming practices E_T can be estimated from class A-pan measurements (Qualimetrics, Inc., Sacramento, USA). The CANEGRO model utilises class A-pan measurements, but can also calculate E_T by making use of one of two models; the Penman-Monteith model (Monteith, 1965) or the Priestley-Taylor model (Priestley and Taylor, 1972). The following three sections will briefly discuss the above mentioned methods.

2.1.3.1. Class A-pan

The class A-pan is a conventional and still popular method used to estimate E_T (McGlinchey *et al.*, 1995). Class A-pan however has a great sensitivity towards micro climatic conditions like soil heat flux, vegetative cover around the pan, painting and management (Smith, 1992: 7). By using a lysimeter, Thompson (1986: 15) could obtain accurate values for E_T and determined ratios between E_T and Class A-pan measurements for various sugarcane stages at Pongola (*27°24' S, 31°35' E, elev. 308m*). The E_T to class A-pan ratios ranged between 0.83 and 0.97. It was noted that these ratios declined over crop age and it was concluded that the class A-pan generally overestimated E_T with an average ratio of 0.906 (McGlinchey, 1996). A fixed adjustment of 0.9 × Class A-pan was therefore assumed for sugarcane crops. Class A-pan measurements and subsequent adjustment factors are site specific (Smith 1992: 7) and are not considered to be the most accurate method to estimate E_T (O'Leary and Connor, 1996).

2.1.3.2. The Penman-Monteith model

Penman (1948) derived a combination equation to determine potential vapour flux density (λE_T) (De Jager and van Zyl, 1989; Allen *et al.*, 1989; Smith, 1992). This equation has been considered the most significant advancement in environmental science for the 20th century (de Jager and van Zyl, 1989). Monteith (1965) later adjusted the Penman equation after accounting for canopy resistance and derived eq. 2.1.7 known as the Penman-Monteith equation. Smith (1992: 6) mentioned that the Penman-Monteith approach is currently viewed as the best-performing combination equation for vapour flux. Thompson (1986) adopted the Penman-Monteith equation to determine E_T for sugarcane. It was later reviewed and incorporated into the CANEGRO sugarcane model (Inman-Bamber *et al.*, 1993; McGlinchey and Inman-Bamber, 1996).

$$\lambda E_T = \frac{\Delta(R_n - G) + \rho C_p(\bar{e}_d)/r_a}{\Delta + \gamma\left(1 + \frac{r_c}{r_a}\right)} \qquad (2.1.7)$$

where λE_T is the potential vapour flux density ($MJ \times m^{-2} \times d$), Δ is the slope of saturated vapour pressure temperature curve ($kPa \times °C^{-1}$), R_n is net radiation flux density to the plant canopy ($MJ \times m^{-2} \times d^{-1}$), G is the soil heat flux ($MJ \times m^{-2} \times d^{-1}$) = $0.21(T_i - T_{i-1})$ where T_i is the mean air temperature on the i^{th} day (McGlinchey and Inman-Bamber, 1996), ρ is the density of air ($kg \times m^{-3}$), C_p is the specific heat of air ($1.0046 \times 10^{-3} MJ \times kg^{-1} \times °C^{-1}$) (ASCE 1990: 284), e_a and e_d are the saturated and measured vapour pressures of the air (kPa), γ is the psychrometric constant for unaspirated conditions, r_a is the average daily aerodynamic resistance to vapour and heat diffusion ($m \times s^{-1}$) (McGlinchey and Inman-Bamber, 1996).

2.1.3.3. The Priestley-Taylor model

A simplified equation to calculate vapour flux density, developed by Priestley and Taylor (1972), was recommended by the ASCE (1990: 100). This equation assumes wet or humid conditions and ignores the aerodynamic component of the Penman-Monteith equation. It is particularly useful when no humidity readings are available.

$$\lambda E_T = \alpha_p \frac{\Delta}{\Delta + \gamma}(R_n - G) \qquad (2.1.8)$$

where α_p is an empirically determined coefficient with α_p=1.095 for sugarcane (Inman-Bamber and Kiker, 1997).

2.2. Soil Properties

The CANEGRO model's soil profile was based on the CERES-Maize model (Jones and Kiniry, 1986: 39-42). This model defines up to ten different horizontal layer compartments, each with different physical characteristics. Most of these characteristics are determined by

the clay, silt and sand contents of the soil, which are based on the soil's particle sizes (see Table 2.1). Clay, silt and sand concentrations are expressed as a percentage of the total volume of the soil.

Table 2.1 Particle sizes determining soil composition (Ritchie *et al.*, 1989).

Soil type	**Particle size range**
Clay	< 0.002 *mm*
Silt	0.002 *mm* – 0.05 *mm*
Sand	0.05 *mm* – 2 *mm*

Other physical characteristics are the layer thickness z_s (*cm*), volumetric soil water content at saturation (*SAT* in $cm^3 \times cm^{-3}$), volumetric soil water content at drained upper limit of plant-extractable water (*DUL* in $cm^3 \times cm^{-3}$) and volumetric soil water content at drained lower limit of plant-extractable water (*LL* in $cm^3 \times cm^{-3}$). The potential plant extractable water in a given soil layer *j* (θ_{EGj} in $cm^3 \times cm^{-3}$) is calculated as the difference between DUL_j and LL_j.

With the exception of soil heat flux (*G* in eq. 2.1.7), water content is the only dynamic soil variable that is currently being simulated by the CANEGRO sugarcane model. Therefore this section will focus on the dynamics of water in two states, those directly above and those within the soil.

Water that accumulates on the soil surface, unable to infiltrate, is called runoff water. In the CANEGRO model, runoff is removed to a sink. Runoff is expressed in the same two-dimensional unit as precipitation and evapotranspiration ($mm^3 \times mm^{-2} \times d^{-1}$). Water infiltrates the soil profile in layers in units of $mm^3 \times mm^{-2} \times d^{-1}$, but is also expressed in $cm^3 \times cm^{-3}$, known as volumetric water content.

Figure 2.1 illustrates the state variable model that is used to simulate water content in and above the soil. Water moves between soil layers j and $j + 1$ at a daily rate ($cm^3 \times cm^{-2} \times d^{-1}$) which is represented by $P_{j,j+1}$. At the same time water can escape from the profile by means of deep infiltration (P_{drain}), root extraction ($R_{we(j)}$), evaporation (E_s) and surface deposition due to saturated conditions (P_{sat}).

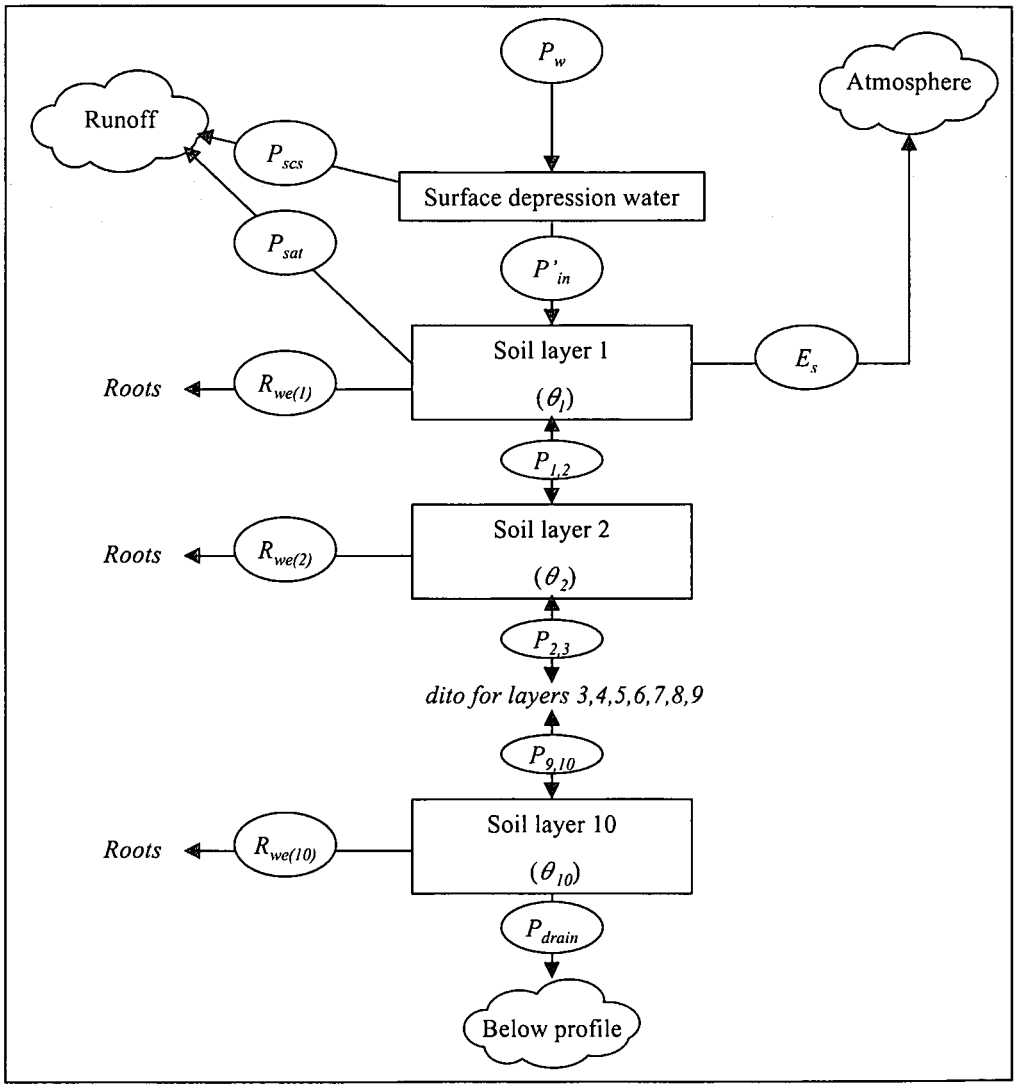

Figure 2.1. A simplified state variable illustration of the CANEGRO runoff and soil water model.

2.2.1. Runoff

Two types of runoff are modelled. (1) Stormflow, which is caused by the soil's infiltration inefficiency and (2) saturated water runoff, which is caused by saturated conditions in the

upper layers of the soil. Runoff is expressed in $mm \times d^{-1}$, which is an abbreviated expression of volume per surface unit ($mm^3 \times mm^{-2} \times d^{-1}$). It affects soil moisture from which plant extractable water can be determined. Runoff can be also used in environmental impact studies to determine soil erosion and pollution.

Stormflow (P_{scs}) only occurs after rain or irrigation. Stormflow is calculated by making use of the U.S. Soil Conversion Service (SCS) curve number method (Jones and Kiniry, 1986: 54). Schulze *et al.* (1992) reviewed this method for South African conditions. P_{scs} is calculated by using the soil's physical characteristics, moisture status and land cover. Schulze *et al.* (1992: Table 2.1) recommended that all soil types be grouped into 4 main and 3 intermediate hydrological categories. An initial response curve number, *CN*, can be allocated to each soil category after considering the current land treatment. This response curve number falls in the range [0, 100] and represents the soil's infiltration response when the volumetric soil water content is at the *DUL* level. *CN* is also adjusted according to the crop's current canopy state (Inman-Bamber and Kiker, 1997) and soil moisture (Schmidt and Schulze, 1987: 35). Jones and Kiniry (1986: 55) calculated the amount of water that will potentially infiltrate the soil (P'_{in}), in $mm^3 \times mm^{-2} \times d^{-1}$, as follows:

$$P'_{in} = P_w - P_{scs} \tag{2.2.1}$$

where P_w ($mm^3 \times mm^{-2} \times d^{-1}$) is the total amount of water added to the crop on a certain day.

Due to the lack of rainfall intensity data it is normally assumed that P_w was evenly distributed over a 24 hour period. The model does not simulate water that was intercepted by particles on the soil surface, like trash.

Total daily runoff can increase due to saturated soil conditions (P_{sat} in Figure 2.1). The CANEGRO model makes use of a comprehensive soil water balance model (see 2.2.2). The

simulation of P_{sat} is better explained in conjunction with the rest of the soil water balance in the following section.

2.2.2. Soil water content

Soil water dynamics can be subdivided into four categories (Wang, 1967: 27):

- Gravitational water that percolates through the soil under the force of gravity.
- Capillary water that moves toward the region of greatest capillary tension, regardless of gravitational direction.
- Hygroscopic water that remains in the soil and is not influenced by the above two factors.
- Combined water that is chemically captured and remains after the hygroscopic water has evaporated. This is held by chemical combination.

The CERES-Maize water balance as described by Jones and Kiniry (1986) was adjusted by Inman-Bamber (1991) to accommodate sugarcane growth requirements. This model is unidimentional along a vertical axis and calculates volumetric soil water content (θ in $cm^3 \times cm^{-3}$) for each soil layer on a 24 hour time step (van Antwerpen, 1998: 5-6). Four mechanisms are simulated in the following sequence; (1) gravitational flow, (2) soil evaporation, (3) capillary flow (Jones and Kiniry, 1986: 54-61) and (4) water extraction by the root system. The first three of these mechanisms will be discussed briefly in the following sections. Root extraction will be discussed in 3.4.

2.2.2.1. GRAVITATIONAL FLOW

Gravitational flow takes place when the soil layer is relatively wet ($\theta > DUL$). Figure 2.2 illustrates an analogy of the mechanism used to conceptualise gravitational flow conditions.

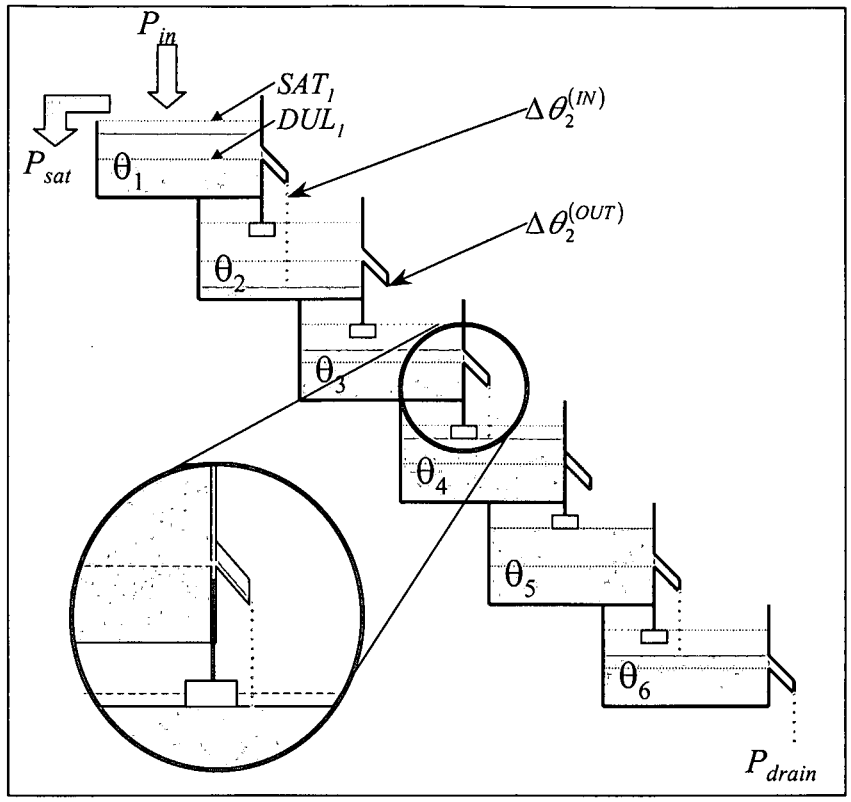

Figure 2.2. An Analogy of the gravitational flow mechanism. Soil levels 2 – 6 have negative feedback to their predecessors, while an overflow in level 1 causes saturated runoff (P_{sat}). Level 5 is in a saturated state and thereby closed the outflow of level 4.

According to the mechanism illustrated in Figure 2.2, the volumetric soil water content at any time t for soil layer j ($\theta_j(t)$ in $cm^3 \times cm^{-3}$) can be calculated by either a continuous or discrete differential equation.

$$\theta_j(t) = \int_0^t \frac{d\theta_j}{dt} dt \tag{2.2.2}$$

$$\theta_j(t) = \theta_j(t-1) + \Delta\theta_j \tag{2.2.3}$$

Jones and Kiniry (1986: 55-57) applied the discrete approach (eq. 2.2.3) with a 24 hour time step and the net flow rate ($\Delta\theta_j$ in $cm^3 \times cm^{-3} \times d^{-1}$) was calculated as the difference between the incoming and outgoing rates ($\Delta\theta_j^{(IN)}$ and $\Delta\theta_j^{(OUT)}$).

$$\Delta\theta_j = \Delta\theta_j^{(IN)} - \Delta\theta_j^{(OUT)} \tag{2.2.4}$$

with

$$\Delta\theta_j^{(IN)} = \begin{cases} \Delta\theta_{j-1}^{(OUT)} \mid \theta_j(t-1) < SAT_j \\ 0 \quad \mid \theta_j(t-1) = SAT_j \end{cases} \tag{2.2.5}$$

The outgoing rate for a specific layer is calculated by making use of a constant drainage fraction coefficient. This coefficient (c_j) is unitless and represents the fraction of the drainage volume for layer j that percolates during each time step (van Antwerpen, 1998: 6). A value for c_j can be established from comprehensive soil analysis. Ritchie *et al.* (1989) suggested different values for c_j, based on soils with different permeabilities.

$$\Delta\theta_j^{OUT} = \begin{cases} c_j\left(\theta_j(t-1) - DUL_j\right) \mid \left(\theta_j(t-1) = SAT_j;\ \theta_j(t-1) \geq DUL_j + 0.00\right. \\ 0 \end{cases} \tag{2.2.6}$$

Water is added to saturated surface runoff (P_{sat}) when θ_l-$\Delta\theta_l^{(OUT)} > SAT_l$.

2.2.2.2. CAPILLARY FLOW

Capillary flow between soil layers is calculated only after gravitational flow and soil evaporation (see 2.2.2.3). Capillary flow is based on soil water diffusivity. Hillel (1982: 114-116) derived a soil water flux equation by defining hydraulic diffusivity (D_θ) as the ratio of the water flux (θ_D) to the soil water content gradient over depth.

$$\theta_D = -D_\theta \frac{\partial\theta}{\partial z} \tag{2.2.7}$$

where (z in cm) is soil depth.

If eq. 2.2.7 is applied for daily iterations, the hydraulic diffusivity will be expressed in $cm^2 \times d^{-1}$, the rate of change in θ over depth will be expressed in $cm^3 \times cm^{-3} \times cm^{-1}$, water flux will be expressed in $cm^{-3} \times cm^{-2} \times d^{-1}$.

Jones and Kiniry (1986: 60-61) used a discrete form of this approach to determine the daily water flux between layers j and $j+1$ ($\theta_{D(j,\,j+1)}$ in $cm^3 \times cm^{-3} \times d^{-1}$). $\theta_{D(j,\,j+1)}$ represents the water

flux from soil layer $j+1$ to j and will be negative if the flux is in the opposite direction. The model is applied from the top to the bottom layers and ignores the first soil layer if $z_{s(1)}<5cm$. Figure 2.3 illustrates an analogy for this diffusivity mechanism.

$$\theta_{D(j,\ j+1)} = D_\theta m_{j,\ j+1} \tag{2.2.8}$$

where

$$D_\theta = 0.88e^{\left(35.4\times\frac{z_{s(j)}\theta'_j + z_{s(j+1)}\theta'_{j+1}}{2(z_{s(j)}+z_{s(j+1)})}\right)} \tag{2.2.9}$$

and

$$m_{j,\ j+1} = \left(\frac{\theta'_{j+1}}{\theta_{E(j+1)}} - \frac{\theta'_j}{\theta_{E(j)}}\right)\left(\frac{z_{s(j+1)}\theta_{E(j+1)} + z_{s(j)}\theta_{E(j)}}{z_{s(j+1)} + z_{s(j)}}\right)\left(\frac{1}{\frac{1}{2}\left(z_{s(j+1)} + z_{s(j)}\right)}\right) \tag{2.2.10}$$

with $z_{s(j)}$ the thickness of layer j (cm), $\theta'_j=\max\{\theta_j - LL_j, 0\}$ and $\theta_{E(j)}=DUL_j - LL_j$ in $cm^3\times cm^{-3}$.

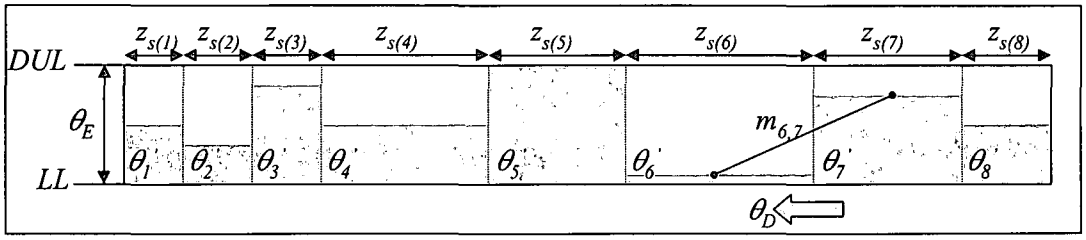

Figure 2.3. An analogy mechanism for soil capillary flow. Water compartments are separated by flow restricting membranes.

2.2.2.3. SOIL EVAPORATION

Soil moisture evaporation below a transpirating plant canopy (E_s), expressed in $mm^3\times mm^{-2}\times d^{-1}$, is calculated in order to establish the evapotranspiration deficit that drives the crop's transpiration rate (Ritchie and Burnett, 1971). Potential soil evaporation (E_{ps}) is the amount of water that will evaporate from the soil if the soil surface remains wet. E_{ps} will decrease with crop age due to surface shading (ASCE, 1990: 50). Jones and Kiniry (1986) used the crop's leaf area index (LAI) to calculate E_{ps} as a fraction of E_T. Inman-Bamber (1991) argued that dry sugarcane leaves will continue to shade the soil and should thereby be included in the calculation of LAI.

$$E_{ps} = \begin{cases} E_T\left(1 - 0.43 LAI_{tot}\right) & LAI_{tot} \le 1 \\ \dfrac{E_T}{1.1 \times e^{\left(-0.4 LAI_{tot}\right)}} & LAI_{tot} > 1 \end{cases} \qquad (2.2.11)$$

where LAI_{tot} (eq. 3.2.7) is the total leaf area index of dry and green leaves.

Jones and Kiniry (1986: 53, 60) assumed that soil evaporation takes place in the first soil layer only. The combined water content after hygroscopic water extraction was assumed to be a constant fraction of the lower limit of plant extactable water, $f_{01} \times LL_1$, with

$$f_{01} = 0.9 - 3.8 \times 10^{-4}\left(z_{s(1)} - 30\right)^2 \qquad (2.2.12)$$

where $z_{s(1)}$ (cm) is the thickness of the first soil layer.

Philip (1959) identified two stages of soil surface evaporation; *(1)* wet soil surface and *(2)* drying soil surface. Stage 1 is limited by the heat energy available, the soil's depth and hydraulic properties, while stage 2 is more controlled by the soil specific hydraulic conductivity (ASCE, 1990: 48). The model uses a critical value (U in $mm^3 \times mm^{-2}$) that represents the maximum amount of water that can freely evaporate from the soil. U is a soil dependant parameter, which can be derived from the albedo (Jackson *et al.*, 1976) and sand and clay content (Ritchie *et al.*, 1989). Jones and Kiniry (1986: 58-60) addopted this appraoch in their water balance.

Overall, the environmental aspects of the CANEGRO sugarcane model represent well tested concepts and functions with special adaptions for sugarcane.

Chapter 3

THE CROP ASPECTS OF THE CANEGRO SUGARCANE MODEL

3.1. Introduction To The Crop Properties

This chapter deals with plant related properties that are modelled in the CANEGRO sugarcane model. The primary driving forces of the various processes taking place in the individual plant and the crop as a whole will be discussed. Although the availability of water plays an important role in most physiological processes, it was regarded more important to describe the system firstly in the absence of water stress. Influences by water stress are briefly dealt with towards the end of this chapter.

A tiller is the smallest individual and self-sustainable unit in a sugarcane crop. Although roots can be commonly shared among tillers, each tiller consists of a single stalk with a number of leaves. Sugarcane as an individual tiller and as a crop undergoes various changes over time. Since the CANEGRO model attempts to simulate the agricultural production system, crop phases and characteristics are of more importance than individual tiller characteristics. In modelling this it was however necessary that some of the physiological processes and characteristics of the individual tillers be understood and simulated before the crop could be represented. This overview firstly deals with the description of the individual tiller characteristics. After that, tiller characteristics could be extrapolated to produce descriptive parameters for the crop as a whole.

Photosynthesis is the most important process in the production system of the plant. Photosynthesis has been better described in the broader sense of the crop's production and

was divorced from individual tiller characteristics (Thornley, 1976: 92-122; Thompson, 1978; Inman-Bamber, 1991). Due to practical difficulties, studies on the root system also favoured a holistic approach, thus ignoring individual tillers. The biomass accumulation model and rooting system model could therefore only be discussed after the tiller and crop characteristics were well defined.

3.2. Phenology, Tiller and Crop Characteristics

3.2.1. TILLER POPULATION

Tiller density, also generally known as population (n_{pop} in $tillers \times ha^{-1}$) is an important crop variable that is simulated by the CANEGRO model. It is later used to determine the amount of radiation flux that was intercepted by the crop, which is an important factor in determining photosynthesis and transpiration.

Some agricultural practices and biological processes can influence tiller population. Planting and harvesting practices like row spacing and planting density (e.g. Kanwar and Sharma, 1974) and mechanical harvesting and in-field haulage (e.g. Cochran and Richaud, 1980) influence tiller population. Three biological processes in sugarcane influence tiller population. Those are (1) the germination and emergence of primary tillers, (2) the natural process of underground branching and emergence of secondary and higher order tillers and (3) tiller senescence. Under suitable growing conditions a typical commercial crop's tiller population will increase rapidly, which will then be followed by a phase of tiller senescence before the population becomes more stable.

Rostron (1972) found that tiller numbers could be correlated with cumulative heat units. Inman-Bamber (1994b) also noted that tillering rates, which is the rate at which underground branching occurs, could be mathematically linked to leaf emergence rates (see 3.2.2.1).

Inman-Bamber (1994b) concluded that heat units with a base temperature of 16°*C* produced the best results when compared with observed tiller populations. Tiller population was subsequently calculated by making use of a difference equation.

$$n_{pop}(t) = n_{pop}(t-1) + \Delta_{pop} \tag{3.2.1}$$

where t is time in days and Δ_{pop} ($tillers \times ha^{-1} \times d^{-1}$) is the change in the tiller population since the previous day.

The simulated crop's population reaches a peak at 500°$C \times d$ (base 16°*C*). It was assumed that tillers exceeding the population of $3 \times 10^5 tillers \times ha^{-1}$ would be small enough to be ignored (Inman-Bamber and Kiker, 1997). Four ΣHU_{16} intervals were identified to calculate Δ_{pop}, those were $\Sigma HU_{16} \in$ (0, 600°$C \times d$), [600, 1500°$C \times d$], (1500, 2000°$C \times d$) and [2000, ∞°$C \times d$). For the intervals $\Sigma HU_{16} \in$ [0, 600°$C \times d$] and $\Sigma HU_{16} \in$ (600, 1500°$C \times d$) the derivative of a 2nd order polynomial was used (Inman-Bamber and Kiker, 1997).

$$\Delta_{pop} = \left(1000 \times \frac{1.4}{z_{row}}\right)\left(p_1^{(cul)} + 2p_2^{(cul)}\Sigma HU_{16}\right)\left(HU_{16}\right) \quad \left|\Sigma HU_{16} \leq 1500°C\right. \tag{3.2.2}$$

where z_{row} (m) is the row spacing, $p_i^{(cul)}$ are cultivar specific polynomial coefficients (see Table 3.1.) and HU_{16} is the heat units for the current day (°$C \times d$).

Inman-Bamber (1991) noted that a mature sugarcane crop would have a predictable tiller population. These populations differ among cultivars, as summarised in Table 3.2. Although it was later considered that seasonal effects may play a role in mature tiller populations (Inman-Bamber, 1994a), the CANEGRO model assumes a fixed mature tiller population. Tiller senescence would slow down after 1500°$C \times d$ and a linear decline towards the mature tiller population was maintained in the interval $\Sigma HU_{16} \in$ (1500, 2000°$C \times d$). The population is kept constant after 2000°$C \times d$ for the rest of the duration of the crop.

Table 3.1. 2nd order polynomial coefficients that were used to calculate $\Delta_{p\times p}$ for different cultivars in the intervals $\Sigma HU_{16} \in (0 - 600°C\times d)$ and $\Sigma HU_{16} \in [600 - 1500°C\times d]$ (Inman-Bamber and Kiker, 1997).

	$\Sigma HU_{16} \in (0 - 600°C\times d)$		$\Sigma HU_{16} \in [600 - 1500°C\times d]$	
	p_1	p_2	p_1	p_2
NCo376	1.8260	-0.00201	-0.9902	3.282×10^{-4}
N12	0.01365	35.6594	3.689×10^{-3}	-7.260×10^{-6}
N14	-44.7707	40.5385	4.944×10^{-3}	-1.080×10^{-5}
R570	-38.4800	0.3190	-2.253×10^{-9}	1.019×10^{-11}

Table 3.2 Mature tiller populations for different cultivars.

Cultivar	**Mature tiller population** ($tillers\times ha^{-1}$)
NCo376	*133 000*
N12	*150 000*
N14	*120 000*
R570	*80 000*

Because tillering is a continuous process for a certain duration of the crop, the CANEGRO model accounted for inhomogeneous tillers by simulating up to thirty cohort groups while the crop is still in its developmental stages. Once the crop reaches its mature tiller population, cohort groups are combined into one group of homogenous tillers. Van Dillewijn (1952: 83-86) noted that higher order tillers differ in vegetative composition to the primary tillers. Although limited data exist to investigate these differences it could be anticipated that future refinements to the model could include this issue.

The simulation of tiller population is based on empirically fitted polynomial equations and does not follow a mechanistic approach. The absence of a mathematical description of the three biological processes that influence tiller population limits the model's ability to simulate different planting and harvesting practices, like high density and double stick planting,

ratooning and in-field mechanisation. The CANEGRO model will therefore enhance its functionality if future versions could simulate tiller emergence, tillering and tiller senescence in a more mechanistic way.

3.2.2. Leaf emergence and development

3.2.2.1. LEAF EMERGENCE

Under water stress free conditions, leaves will emerge according to a defined phyllochron interval (Inman-Bamber, 1994b). A phyllochron interval, expressed in $°C \times d$, is a specific amount of heat units that need to lapse before the next leaf on a tiller will emerge. Inman-Bamber (1994b) based the phyllochron interval on heat units with base $10°C$ and determined a fixed phyllochron interval for the first 14 leaves (ξ_1) and another for leaves emerging thereafter (ξ_2). This is generally referred to as the broken stick equation. Van Antwerpen (1999) noted that higher biomass allocation rates to the rooting system could be one of the reasons for a change in the phyllochron interval after the 14th leaf.

$$n_{leaf} = \begin{cases} 1 + \dfrac{\Sigma HU_{10}^{(1)} - \Sigma HU_{10}}{\xi_1} & \left| \; \Sigma HU_{10}^{(1)} - \Sigma HU_{10} \le 13\xi_1 \right. \\ 15 + \dfrac{\Sigma HU_{10}^{(2)} - \Sigma HU_{10}}{\xi_2} & \left| \; \Sigma HU_{10}^{(1)} - \Sigma HU_{10} > 13\xi_1 \right. \end{cases} \tag{3.2.3}$$

where n_{leaf} is the number of leaves per stalk, $\Sigma HU^{(1)}_{10}$ is the accumulated heat units since the emergence of the tiller, and $\Sigma HU^{(2)}_{10}$ is the accumulated heat units since n_{leaf} reached a value of 14. Table 3.3 reflects different phyllochron intervals for different cultivars.

The senescence of green leaves in the CANEGRO model was based on the NCo376 cultivar. It was assumed that this cultivar would never have more than 12 green leaves at any stage.

Table 3.3. Phyllochron interval for different cultivars (Inman-Bamber, 1994b; Inman-Bamber and Kiker, 1997).

Cultivar	ξ_1 (°C×d)	ξ_2 (°C×d)
NCo376	109	169
N12	118	200
N14	109	169
R570	119	119

3.2.2.2. LEAF DEVELOPMENT

Inman-Bamber (1994b) found the daily leaf elongation rate (E), expressed in $mm \times d^{-1}$, to be dependent on air temperature. A linear function was fitted on hourly-recorded leaf elongation data to determine a relationship with the mean daily temperature ($\overline{T}$ *in* °C×d).

$$E = 24 \times \left(-1.77 + 0.176\overline{T} \pm 0.45\right) \tag{3.2.4}$$

In the model it is assumed that no more than 4 leaves can expand simultaneously. Older leaves stop expanding once they reach a maximum allowable blade area. The maximum allowable blade area ($A_{max(j)}$ *in* cm^2) for the j^{th} sequential leaf since emergence is assumed to be leaf number and cultivar specific (Inman-Bamber and Kiker, 1997). Eq. 3.2.5 reflects the calculation of $A_{max(j)}$ for the NCo376 cultivar.

$$A_{max(j)} = \begin{cases} -20.8 + 27.2j & |j \le 15 \\ 387.2 & |j > 15 \end{cases} \tag{3.2.5}$$

More information on similar equations for other cultivars and leaf size properties are listed in Appendix A.

3.2.2.3. LEAF AREA INDEX AND LIGHT INTERCEPTION

The fraction of light intercepted by the crop is determined by the leaf area index. Leaf area index is a measure of the crop's canopy and describes the relative collective area of foliage over all the tillers in the crop. Two parameters, the number of tillers and the total leaf area per tiller therefore determine the light interception ability of the canopy.

Leaf area index (LAI in $cm^2 \times cm^{-2}$) is the total green leaf area per unit land surface. Leaf area index incorporates all the tillers on a unit surface and thereby represents characteristics about the crop as a whole, irrespective of the various states of different tillers. LAI can be calculated from the mean leaf area per tiller, $\overline{LA}$ (cm^2), and tiller population, n_{pop} ($tillers \times ha^{-1}$).

$$LAI = \overline{LA} \times n_{pop} \times 10^{-8} \tag{3.2.6}$$

Inman-Bamber (1991) explained that dead leaves, which are not inclusive of LAI, would continue to shade the soil and therefore included this into the soil evaporation model (eq. 2.2.11). The total leaf area index of dead and green leaves, LAI_{tot} ($cm^2 \times cm^{-2}$) was calculated by accumulating $A_{max(j)}$ over the different simulated cohort groups. This approach does not account for leaf rolling and shrinking that take place when leaves die (Inman-Bamber and Kiker, 1997).

$$LAI_{tot} = LAI + \sum_{k=1}^{K} \sum_{j=1}^{J_k} A_{\max(j)} \tag{3.2.7}$$

where K is the number of cohort groups in the CANEGRO model and J_k is the number of dead leaves per tiller in the k^{th} cohort group.

Bouman *et al.* (1992) highlighted the importance of knowing the proportion of ground that is shaded by the crop. This property can be used to determine radiation interception and photosynthesis. By making use of LAI Inman-Bamber (1994b) calculated the fraction of PAR

that was intercepted by the crop. This is known as the light interception of the canopy (L_i) and is calculated by making use of Beer's law.

$$L_i = 1 - e^{-ki \cdot LAI} \tag{3.2.8}$$

where *ki* is the extinction coefficient, which reflects properties of the canopy structure and time of the day.

Muchow *et al.* (1982) suggested that the value for *ki* changes during the developmental stages of the crop. In the CANEGRO model *ki* varies from 0.58 to 0.84 and is expressed as a function of the number of leaves in the first cohort group ($n_{leaf(1)}$).

$$ki = \begin{cases} 0.58 + 0.26\dfrac{n_{leaf(1)}}{20} & \mid n_{leaf(1)} \le 20 \\ 0.84 & \mid n_{leaf(1)} > 20 \end{cases} \tag{3.2.9}$$

3.2.3. Stalk height and canopy height

In the CANEGRO model stalk height (z_{stk} in *cm*) was assumed to increase at a rate of 16% of daily leaf elongation (eq. 3.2.4). Stalk height is calculated for each tiller cohort group. Inman-Bamber (1994a) noted that stalk growth would slow down once the tiller reached maturity. Van Dillewijn (1952: 81-87) also pointed out that tillers of a higher order (i.e. later emerging tillers) would elongate faster than primary tillers. It was further noted that at a distinct stage in the crop, tillering would slow down and stalks would elongate more rapidly. These characteristics have not been considered for the CANEGRO model yet. They could form part of future model refinements.

Canopy height (z_{can} in *cm*) was calculated by assuming a 30.2° angle between the stalk and the tip of the highest leaf.

$$z_{can} = z_{stk} + \cos(30.2°) \times l \tag{3.2.10}$$

where *l* (*cm*) is the length of the longest leaf in the first tiller cohort group.

3.3. Photosynthesis, Respiration and Partitioning

Photosynthesis and respiration are based on carbon exchange. The crop's weight in the absence of water, also known as dry weight (W), is normally associated with a carbon model. W is known as the plant's biomass and is comprised of the plant mass above the ground (W_a), also known as aerial biomass, and the plant mass under ground (W_r). The aerial biomass includes the mass of green foliage (W_l), the stalk (W_s) and dead plant material (W_t), known as trash. Figure 3.1 illustrates these different plant components. All biomass entities are expressed in $t \times ha^{-1}$.

3.3.1. Photosynthesis

Photosynthesis is the process by which carbohydrates (CH_2O) are synthesised from carbon dioxide and water. This is done by chlorophyllous cells in the presence of light (Meyer *et al.*, 1960: 193). The following simplified chemical equation summarises the general concept of photosynthesis and respiration.

$$6CO_2 + 6H_2O \underset{\text{Respiration}}{\overset{\text{Photosynthesis}}{\rightleftharpoons}} 6(CH_2O) + 6O_2\uparrow \qquad (3.3.1)$$

Photosynthesis has a convex, asymptotic response to light absorption (Spitters *et al*, 1986) and was assumed to only take place when the crop has adequate leaves ($LAI > 1 \times 10^{-3} cm^2 \times cm^{-2}$). Various models have been developed to simulate photosynthesis (e.g. Thornley, 1976:93-110; CSSA, 1991). Inman-Bamber and Thompson (1989) used a photosynthesis application of Mishoe *et al.* (1979), which was based on the work of Hesketh *et al.* (1971). The model calculates the gross photosynthesis (P_g in $t\ CH_2O \times ha^{-1} \times d^{-1}$) on a crop level. Assuming that the caloric value of dry matter is $17.556 MJ \times g^{-1}$, P_g is calculated according to eq. 3.3.2.

$$P_g = L_i \times \varepsilon \times \left(\frac{100}{17.556} PAR \right) \tag{3.3.2}$$

where ε, which is a fraction, is the gross photosynthesis efficiency and L_i is the fraction of light that was intercepted by the crop (eq. 3.2.8).

Inman-Bamber and Thompson (1989) reported the efficiency of gross photosynthesis (ε) to vary between the values of 0.082 and 0.088 with regard to crop age and season. Inman-Bamber (1995b) noted that these values excluded a respiration component and assumed a constant value of 0.12.

3.3.2. Respiration

Inman-Bamber and Thompson (1989) applied a respiration model, based on the work of Lorber *et al.* (1984), to South African sugarcane production conditions. This model functions on a crop level and doesn't attempt to simulate differences between tillers. The model divided respiration into two processes, maintenance respiration and growth respiration. Inman-Bamber (1991) concluded that this approach was adequate for predicting dry matter accumulation.

The maintenance respiration fraction (R_m) is the allocated fraction of CH_2O that is required to sustain existing plant matter. Hesketh *et al.* (1971) assumed this to be proportional to the plant's accumulated biomass. The remainder of CH_2O was then to be allocated to growth, of which some would be converted to plant matter (ΔW in $t \times ha^{-1} \times d^{-1}$) and some respired during the growth process. Lorber *et al.* (1984) assumed growth respiration to be a constant fraction (R_{gr}) of the remaining CH_2O after maintenance respiration.

$$\Delta W = \left(P_g - R_m W \right) \left(1 - R_{gr} \right) \tag{3.3.3}$$

where W is the accumulated dry mass of the crop ($t \times ha^{-1}$).

The maintenance respiration fraction was found to be 0.003 of the existing plant dry mass, while the growth respiration fraction was 0.242 of the remainder of the daily CH_2O after maintenance (Inman-Bamber and Thompson, 1989). These values were calibrated on irrigated crops with little water stress for the NCo376 cultivar. The relatively low maintenance respiration fraction was confirmed under non-irrigated conditions during later experiments (Inman-Bamber, 1994a). In the CANEGRO sugarcane model a maintenance respiration fraction of 0.004 is used.

These respiration processes were calculated as fractions of the biomass (W), which included trash (W_t). In the event of a low photosynthesis rate ($P_g<R_mW$), existing soluble CH_2O of the plant can be utilised for maintenance respiration. This is called negative growth and was assumed to occur only after the crop accumulated more than $5t \times ha^{-1}$ dry mass. Eq. 3.3.3 was applied without any adjustment during negative growth. This included the calculation of a growth respiration component ($1-R_{gr}$), when no growth was actually taking place.

3.3.3. Dry matter allocation

During the growth process, new dry matter (ΔW) is allocated to different organs of the plant. Thornley (1976: 152-171) developed models to partition ΔW into the various plant organs. Thompson (1978) indicated rates at which organs develop during the life-cycle of the sugarcane tiller. Roots initially develop fast when the plant is still young, leaves and stalk growth only accelerates at a later stage. Inman-Bamber (1994a) noted that due to respiration losses and a decline in LAI, growth would normally slow down after the crop has reached an age of ten months.

Van Dillewijn (1952: 162-168) noted that at an age of 12 months, 88% of all biomass is above ground. Inman-Bamber and Thompson (1989) derived various relationships between the different aerial biomass organs. Figure 3.1 illustrates how the partitioning of sugarcane is

mathematically represented. In the CANEGRO model the fractional allocation of new biomass to different organs is driven by the current accumulated biomass. Van Antwerpen (1998: 44-53) reviewed the relationships between root biomass and aerial biomass. The fraction of biomass allocated to roots (f_r) is calculated according to Inman-Bamber (1991).

$$f_r = c_a + \frac{1}{c_b + c_c W} \tag{3.3.4}$$

where c_a, c_b and c_c are empirically calibrated coefficients with values 0.1, 1.8 and 0.05 respectively.

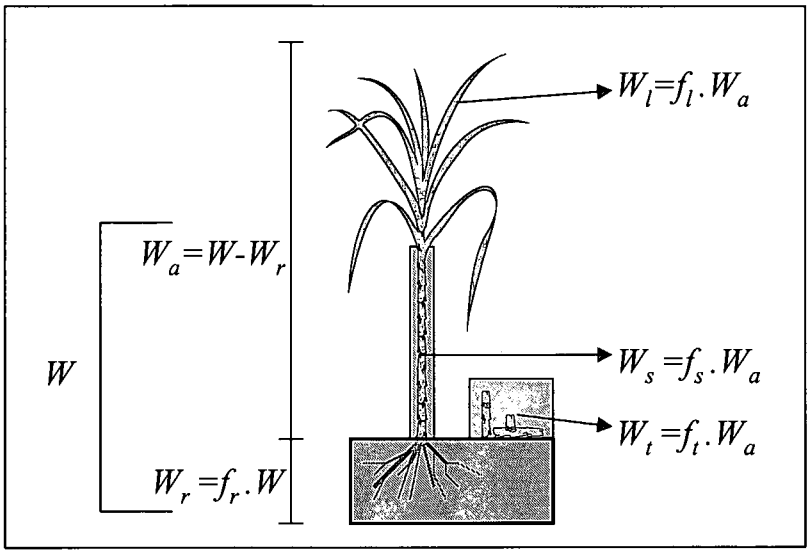

Figure 3.1. A mathematical representation of the partitioning of sugarcane.

The fraction of biomass allocated to green leaves (f_l) is allowed to vary between 5 and 100% of W_a. A 3rd order polynomial function is used to express f_l in terms of W_a (Inman-Bamber and Thompson, 1989).

$$0.05 \le f_l = 1.06 - 0.051 W_a + 9.344 \times 10^{-4} W_a^2 - 5.691 \times 10^{-6} W_a^3 \le 1.0 \tag{3.3.5}$$

The fraction of aerial biomass allocated to the stalk (f_s) is calculated by the following combined function (Inman-Bamber and Kiker, 1997):

$$f_s = \begin{cases} 0 \le -0.03 + 0.0256 W_a \;\middle|\; W_a \le 18.5 t \times ha^{-1} \\ 0.72 - e^{(-0.04777 W_a - 0.4105)} \;\middle|\; W_a > 18.5 t \times ha^{-1} \end{cases} \tag{3.3.6}$$

The remainder of aerial biomass is regarded as trash.

$$f_t = 1 - f_s - f_l \tag{3.3.7}$$

The allocation of carbon to the different plant organs was determined according to the accumulated mass ratios between these organs. Because it is not driven by external factors, like temperature, this approach could limit some applications of the CANEGRO model. Leaf elongation rate (eq. 3.2.4) suggests that carbon allocation to foliage could be temperature driven. Unpublished work suggests a specific leaf blade area of $25.29 cm^2 \times g^{-1}$ for the NCo376 cultivar (*pers. comm.* R.A. Donaldson, SASA Experiment Station, Mount Edgecombe, South Africa). These results could form part of future model refinements to integrate mass and foliage properties. In a similar way van Antwerpen (1999) suggested that carbon allocation rates to roots could be driven by tiller age. Van Antwerpen (1999) also suggested that the prolonged phyllochron interval after the 14th leaf (eq. 3.2.3) could imply higher carbon allocation rates to the root system.

3.3.3.1. PARTITIONING TO SUCROSE

Due to the high commercial value of sugar, the fraction of sucrose in the stalk (f_{suc}), also known as sucrose content, is of great economic interest. Sucrose content has been noted to be dependent on the time of the year, age, cultivar, flowering of the plant and current growth rate (van Dillewijn, 1952: 320-323). The CANEGRO model also simulates substantial differences in sucrose content between irrigated and non-irrigated sugarcane. It is only assumed that the stalk would contain sucrose once $W_s > 2.5 t \times ha^{-1}$. Two functions are used to calculate f_{suc} for irrigated and non-irrigated conditions respectively (eq. 3.3.8).

$$f_{suc} = \begin{cases} irrigated: \\ 0.3386 + 2.308\times10^{-3} W_s + 0.04519\left(\sin\dfrac{t_d}{57.3}\right) \\ non-irrigated: \\ 0.288 + 0.00530 W_s - 3.59\times10^{-5} W_s^2 + 0.0535\left(-\sin\dfrac{t_d - 10}{57.3}\right) + 1.153\times10^{-4} t \end{cases} \quad (3.3.8)$$

where t_d is the day number of the year and t is the age of the crop in days.

Sucrose mass (W_{suc}), expressed in $t\times ha^{-1}$, is then calculated as follows:

$$W_{suc} = f_{suc} \times W_s \quad (3.3.9)$$

3.4. The Root System

Root equations from the CERES-Maize model (Jones and Kiniry, 1986: 62-65) were used to simulate the sugarcane root system. Robertson *et al.* (1993) gave a comprehensive overview of this model's root components and emphasised the importance to accurately simulate root distributions. The CANEGRO model simulates rooting depth and rooting density for each soil layer on a daily basis. Rending and Taylor (1989) identified the following factors that influence root growth: root length, soil water content, soil-plant water potential, hydraulic conductivity and the soil-to-plant pathway.

The daily fraction of ΔW allocated to roots was assumed to be equal to f_r (eq. 3.3.4). Root dry mass is converted to root length per unit surface (L), expressed in $cm\times cm^{-2}$, by making use of a root length to mass ratio (Lm in $cm\times g^{-1}$). The daily amount of root growth (ΔL in $cm\times cm^{-2}\times d^{-1}$) is then calculated as follows (Inman-Bamber and Kiker, 1997):

$$\Delta L = \left(\frac{1}{100} \times f_r \times \Delta W\right) Lm \quad (3.4.1)$$

Root length to mass ratios were found to be dependent on various factors ranging from the soil type to the plant's developmental stage (van Antwerpen *et al.*, 1993; Anderson, 1987; Barber, 1971). Van Antwerpen *et al.* (1993) produced results for the NCo376 cultivar with *Lm* values ranging from 811 to 470 $cm \times g^{-1}$. Van Antwerpen (1998: 51) confirmed that sugarcane has finer and longer roots than maize and reported an average value of $Lm=727 cm \times g^{-1}$. The current value for *Lm* is based on the average results of van Antwerpen *et al.* (1993) of $500 cm \times g^{-1}$.

Jones and Kiniry (1986: 62) noted that rooting depth could be determined from the amount of heat units to which the plant was exposed. The daily rooting depth increment ΔLd ($cm \times d^{-1}$) was therefore assumed to be driven by heat units with a base of 10°C.

$$\Delta Ld = 0.22 HU_{10} \tag{3.4.2}$$

Rooting depth can not exceed the depth of the soil's profile. Van Antwerpen (1998: 53) produced results indicating different rooting penetration rates for soils with different clay contents. Rostron (1974) reported that rooting depth is genetically determined while Gosnell (1971) reported restrictions to root growth due to anaerobic soil conditions. These factors have not been considered in the calculation of rooting depth in the CANEGRO model.

The amount of root growth that will take place in a single soil layer was assumed to be dependant on the existing amount of roots in the layer, the thickness of the layer and the amount of plant extractable water in the layer. Van Antwerpen (1998: 8, 54) noted that root distributions normally decline exponentially with soil depth, but could be highly affected by water availability. If ***F*** is a cumulative distribution function reflecting the distribution of roots in the profile, then the fraction of roots in and below the j^{th} soil layer $w_{R(j)}$ ($cm^3 \times cm^{-3}$) can be calculated from ***F***. Figure 3.2 illustrates these root properties.

$$w_{R(j)} = 1 - \boldsymbol{F}(x_j) \tag{3.4.3}$$

where x_j (cm) is the starting depth of the j^{th} soil layer;

$$x_j = \sum_{k=1}^{j-1} z_{s(k)} \tag{3.4.4}$$

Ritchie *et al.* (1989) assumed for maize that root growth only occurs in the first 200*cm* of the soil profile and suggested the following equation to calculate $w_{R(j)}$.

$$w_{R(j)} = \begin{cases} 1 & | j = 1 \\ e^{\left(-0.02 \times \frac{1}{2}(x_j + x_{j+1})\right)} & | j > 1 \end{cases} \tag{3.4.5}$$

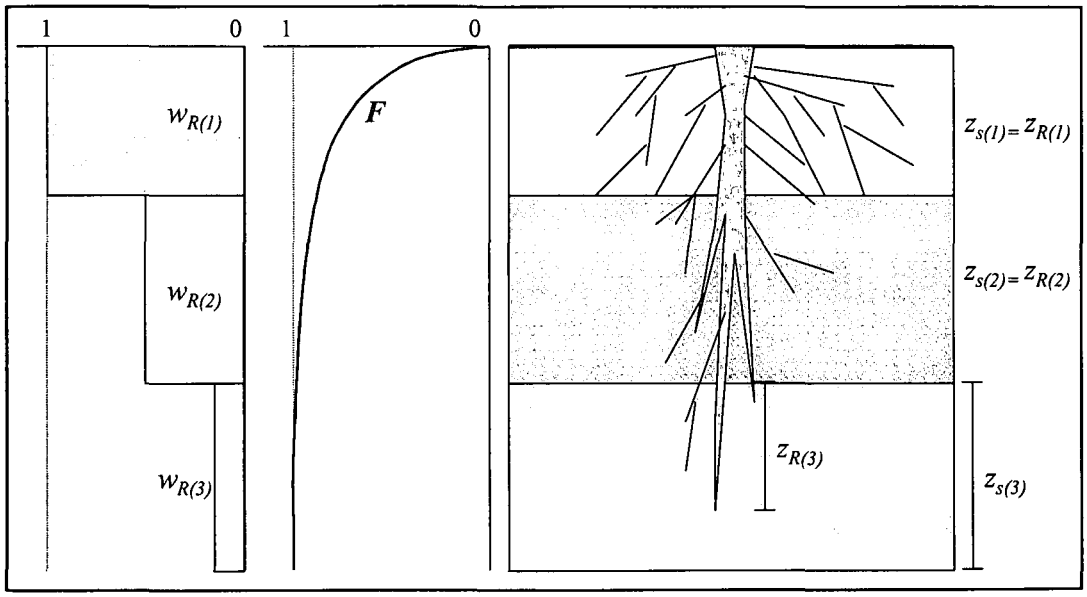

Figure 3.2. An illustration of the root properties that are used to calculate distributed root growth.

Jones and Kiniry (1986: 63-64) assumed a daily senescence rate of 0.5% of existing roots within a single layer for a maize crop. They also restricted existing roots, denoted as Lv_j ($cm \times cm^{-3}$), to fall in the range (0, $5cm \times cm^{-3}$). The fraction of ΔL that would expand into the j^{th} layer (ΔLv_j), also expressed in $cm \times cm^{-3}$, is calculated from a combined equation reflecting root development as well as root senescence (eq. 3.4.6).

$$\Delta Lv_j = \Delta L \times \left(\frac{w_{R(j)} \times z_{s(j)} \times \left(\frac{z_{R(j)}}{z_{s(j)}} \right)}{\sum_{k=1}^{J} w_{R(k)} \times z_{s(k)} \times \left(\frac{z_{R(k)}}{z_{s(k)}} \right)} \right) - 0.005 Lv_j \qquad (3.4.6)$$

where $z_{R(j)}$ (cm) is the thickness interval of the j_{th} layer containing active growing roots (see Figure 3.2), J is the total number of soil layers.

The amount of water that will be taken up by the plant's root system is mainly driven by a water gradient potential between the soil and leaves (Rending and Taylor, 1989). This inherently also incorporates the amount of extractable water in the soil and the distribution of roots in the soil profile.

Root water extraction per root length unit in the j^{th} soil layer, ($R_{wu(j)}$ in $mm^3 \times cm^{-1} \times d^{-1}$), was assumed to never exceed $0.7 mm^3 \times cm^{-1} \times d^{-1}$ (van Antwerpen *et al.*, 1993) and is calculated according to eq. 3.4.7 (Jones and Kiniry, 1986: 64; van Antwerpen, 1998: 9). Van Antwerpen (1998: 11) noted that eq. 3.4.7 is more reliable under moist soil conditions.

$$R_{wu(j)} = \frac{10 SC_1 \times e^{(SC_{2(j)} \theta_E)}}{SC_3 - \ln(Lv_j)} \qquad (3.4.7)$$

where SC_1, $SC_{2(j)}$ and SC_3 are dimensionless soil water constant coefficients.

Values for SC_1 and SC_3 are 0.00132 and 6.67 respectively. $SC_{2(j)}$ is determined from the j^{th} soil layer's lower limit of extractable soil water (LL_j).

$$SC_{2(j)} = \max\{120 - 250 LL_j, 32\} \qquad (3.4.8)$$

The amount of water that is extracted from a soil layer ($R_{we(j)}$ in $mm^3 \times mm^{-2} \times d^{-1}$) is then calculated as follows:

$$R_{we(j)} = 10 \times R_{wu(j)} \times Lv_j \times z_{s(j)} \qquad (3.4.9)$$

The total amount of water that is extracted from the soil $\left(\sum_{j=1}^{J} R_{we(j)}\right)$ is not allowed to exceed the potential evaporative demand on the plant. In that case $R_{wu(j)}$ would be homogeneously reduced by the fraction of water that exceeded E_{pp}.

3.5. Water Stress

Van Antwerpen (1998: 1) noted that due to shallow soils and the absence of irrigation a great portion of South African sugarcane is likely to be exposed to frequent water stress. Inman-Bamber (1986: 1-8) explained various effects of water stress on different sugarcane components. Water stress affects leaf, stalk and root growth, photosynthesis, transpiration and leaf and tiller phenology. Two stress indices are simulated according to Jones and Kiniry (1986: 62) and McGlinchey *et al.* (1995). The indices (f_{S1} and f_{S2}) are mainly derived from the ratio between the total amount of soil water available ($\sum_{j=1}^{J} R_{we(j)}$ in $mm^3 \times cm^{-2} \times d^{-1}$) to the crop's transpiration (E_P in $mm^3 \times mm^{-2} \times d^{-1}$).

$$f_{SX} = \min\left\{1, \frac{\sum_{j=1}^{J} R_{we(j)}}{100 \times X \times E_P}\right\} \tag{3.5.1}$$

where

$$E_P = E_T - E_S - E_I \tag{3.5.2}$$

with E_I ($mm^3 \times mm^{-2} \times d^{-1}$) the amount of intercepted water that can evaporate on a given day and where X (X=1, 2) is the index's sensitivity parameter.

Values of the stress indices vary between 1 and 0, with 1indicating no stress and 0 indicating most severe water stress. The first index (f_{S1}) restricts photosynthesis, while the second index (f_{S2}) restricts cell expansion and the growth of new leaves and stalk tissue. The value of the

value of the second index will be less than 1 when the available root water is less than $2\times E_P$, while the first index is less sensitive and will only be less than one once the available root water falls below $1\times E_P$. It has been noted that these calculations of stress initiate too late and then reduce growth too rapidly (van Antwerpen, 1998: 1).

The CANEGRO model takes water availability into account when tiller emergence is simulated. Tillers could have different root systems, which are not currently taken into account when water stress is simulated. A possible future improvement to the CANEGRO model could be the simulation of water stress on tiller level.

The crop aspects of the CANEGRO sugarcane model comprise largely of empirical functions that describe key processes of phenological development, growth and sucrose accumulation. As such, more mechanistic improvements are possible that will improve the utility of the model in explanatory analysis of sugarcane production. A mechanistic approach widens the applicability of the model beyond South Africa to other sugar production regions of the world.

Chapter 4

A PROPOSED TILLER MODEL

4.1. Introduction

In Chapter 3 (3.2.1) it was noted that the CANEGRO model does not mechanistically simulate the following three biological processes: (1) primary tiller germination and emergence, (2) tillering and (3) tiller senescence. This restricts the model's applicability, for example the model is unable to simulate differences between planted and ratoon crops, mechanically harvested and hand harvested crops and to some extent different planting densities.

Tillering and tiller senescence have been noted by van Dillewijn (1952: 79) and Inman-Bamber (1994b) to be partly driven by the state of the existing canopy. In the CANEGRO model the collective influence of the existing canopy is simulated by leaf area index (*LAI*) and light interception (L_i). With regard to these variables this chapter develops an alternative mechanistic tiller model that could be integrated with the CANEGRO model, or other similar models. The typical life cycle of an individual tiller was used to identify and simulate different crop phases.

The individual sugarcane tiller passes different phenological stages during its life cycle. The bud, which is a miniature stem with its growing point, primordia of leaves and roots, initially remains dormant for a certain period. Germination occurs when the bud breaks open and starts forming a new shoot (van Dillewijn, 1952: 61). The new shoot will elongate towards the surface of the soil and once it has emerged will be known as a primary tiller. After emergence, leaves will develop and the primary tiller will produce secondary tillers. Due to different vegetative compositions younger higher order tillers can be very competitive (van

Dillewijn, 1952: 79-86). Very young tillers will however undergo senescence due to competitive conditions during the later stages of the crop. Tillers can also undergo senescence due to flowering and lodging.

The following 5 crop phases were subsequently defined according to phenological development:

1. Pre-germination phase (crop initiation to germination of the first bud).
2. Pre-emergence phase (bud germination to emergence of the first shoot).
3. Primary tiller emergence phase (first shoot emergence to last primary shoot emergence).
4. Secondary tiller emergence phase (last primary shoot emergence to first tiller senescence).
5. Tiller senescence phase (first tiller senescence to harvest).

4.2. Model description

4.2.1. Model overview

This model calculates the daily change in tiller population by making use of the following parameters from the CANEGRO model: heat units (HU_{10} and HU_{16}), leaf number (n_{leaf}), LAI and L_i. Figure 4.1 illustrates the main variables and relationships that exist in the model. Two new input parameters are required; the initial number of buds prior to germination (n_{popi}) and the ratoon number. The calculation of leaf area per tiller (LA) was simplified by a standard conversion from n_{leaf} to LA. Leaf elongation rate (eq. 3.2.4.) was not included into this model.

Three new parameters were introduced to enable the mechanistic modelling of tiller population: (1) A stool diameter correction factor (s') was required to simulate differences between planted crops with narrow stools, subsequently causing more competition, and ratoon

crops where inter-row radiation was more effectively utilised. (2) A relative tillering rate (n') was introduced to simulate the thermal rate at which existing tillers would undergo underground branching, causing an increase in higher order tiller numbers. (3) A minimum sustainable leaf area per tiller (LA'_{min}) was introduced to simulate competitive conditions in the crop. Tillers with leaf areas lower than LA'_{min} were considered too small to compete for light resources and would undergo senescence.

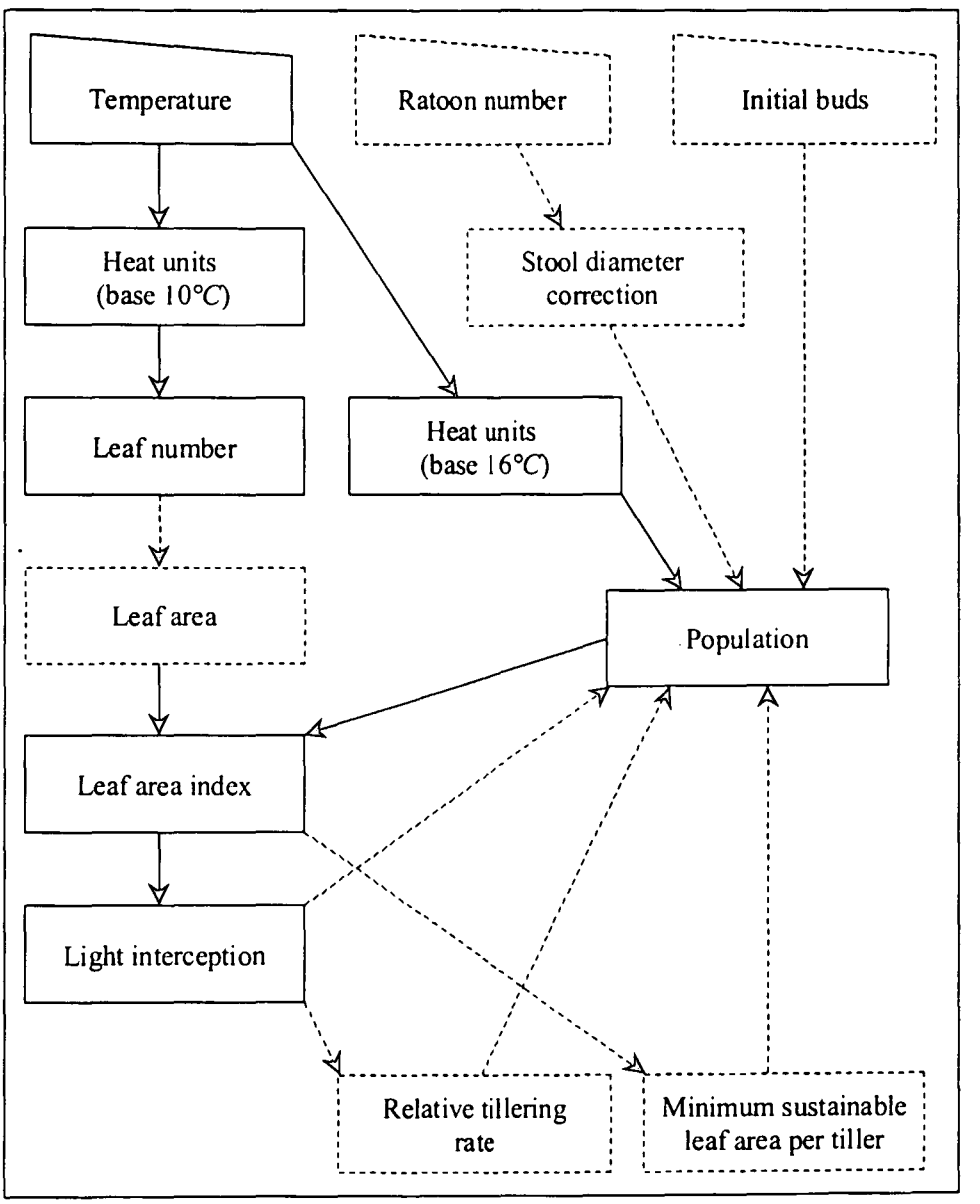

Figure 4.1. Properties and inter-dependencies of the proposed mechanistic tiller model. Properties indicated with solid lines are already simulated in the CANEGRO model while properties indicated with dashed lines were developed for this model.

All the above parameters were sufficient to simulate the different processes during the five crop phases. Crop phases were assumed to be sequential and follow each other without any overlap.

4.2.2. The pre-germination phase

The pre-germination phase starts when the crop is either planted or when the previous ratoon is harvested. During this phase buds remain dormant. Keating *et al.* (1999) calibrated a germination model against HU_9 and suggested a dormant period of $350°C \times d$ for plant crops and $100°C \times d$ for ratoon crops. For consistency with the CANEGRO model, HU_{10} was used and a dormant period of $315°C \times d$ was used for plant crops while $90°C \times d$ was used for ratoon crops.

4.2.3. The pre-emergence phase

Germination constitutes a critical period in the life of the cane plant; a high germination rate means a good start and provides the basis for a sustainable crop (van Dillewijn, 1952: 60-61). This pre-emergence phase starts when the first bud germinates and ends once the first shoot emerges above the ground.

A time lag between germination and emergence accounts for underground growth and depends on the depth and position of the bud. Underground growth is mainly driven by temperature (van Dillewijn, 1952: 66-72; Keating *et al.*, 1999). Keating *et al.* (1999) modelled underground shoot elongation with HU_9 and suggested that $1.250°C \times d$ need to lapse for every $1mm$ growth. For this model $1mm$ underground shoot growth is simulated after every $1.136°C \times d$ of HU_{10}.

4.2.4. The primary tiller emergence phase

During the primary tiller emergence phase tillers appear above the ground and the tiller population increases. Excluding the depth of the bud, emergence above the ground also depends on the position of the bud, length of the cuttings and the presence of sheath (van Dillewijn, 1952: 68-70). The model therefore assumes a fixed duration in HU_{10} for this phase. An estimate of the initial number of buds that will form primary tillers (n_{popi}) is required. This is done by assuming a fixed ratio to the tiller population during the previous ratoon's harvest. Once n_{popi} is known, primary tillers emerge at the specific constant rate that will ensure that all primary tillers have emerged at the end of the fixed duration of this phase.

4.2.5. The tillering phase

Tillering results in a stool of upright stalks containing one primary tiller and various numbers of higher order secondary and tertiary tillers. This process was assumed to be continuous under no resource limitations. Van Dillewijn (1952: 86-87) identified light intensity and day length as the most important driving factors for tillering, while temperature was considered to be the second most important driving factor. It was specifically noted that tillering in sub-tropical regions, like in South Africa, could be particularly sensitive to low temperatures and more extreme day lengths. Inman-Bamber (1994b) noted that HU_{16} could be used to simulate the response of tiller population to temperature.

In this model it is assumed that the tillering phase initiates after the last primary tiller emerged above the ground. Similarly to the CANEGRO model (Inman-Bamber and Kiker, 1997), this model also assumes that younger tillers will undergo senescence first, subsequently causing the tillering phase to terminate as soon as tiller senescence steps in. Van Dillewijn (1952: 81-86) mentioned two fairly distinct sub-phases during tillering; (1) a sub-phase of profuse tillering and (2) a sub-phase with a decline in tillering and more distinctive stalk elongation due to light competition.

Observations during the sub-phase of profuse tillering indicate that the first secondary tiller would emerge above the ground after six leaves on the primary tiller have emerged (unpublished data R.A. Donaldson, SASA Experiment Station, Mt. Edgecombe, 1999). It was assumed that a fixed period is required for the production and emergence of a higher order tiller under no light limitations. This period was defined as the telomechron interval (ω in $°C \times d$). The telomechron interval was derived from the word *telome*, which refers to a terminal branch of a vascular plant (Gray, 1976), and is analogous to the phyllochron interval. This model simulates a constant maximum relative tillering rate in HU_{16} when no light limitations apply (n_ω in $tillers \times tiller^{-1} \times °C^{-1} \times d^{-1}$).

$$n_\omega = \frac{1}{\omega} \tag{4.2.1}$$

The above mentioned conditions imply an exponential increase in tiller population. The population increment per HU_{16} (Δn_{pop} in $tillers \times ha^{-1}$) for this sub-phase can therefore be modelled by a differential equation (Sanches *et al.*, 1988: 104-109).

$$\Delta n_{pop} = n_\omega \times e^{n_\omega(\Sigma HU_{16}+i)} \tag{4.2.2}$$

where ΣHU_{16} ($°C \times d$) is the thermal crop age and i is a fitted constant.

The second sub-phase, which is when light competition exists and stalk elongation receives preference, was assumed to be driven by the light availability to the individual tiller. The model uses L_i and a stool diameter correction factor (s') to determine the amount of competition that exists in the crop. The stool diameter correction factor compensates for recently planted crops to utilise inter-row radiation less efficiently than later ratoon crops. This factor asymptotically approaches 1 for later ratoons. The relative tillering rate under light competitive conditions (n' in $tillers \times tiller^{-1} \times °C^{-1} \times d^{-1}$), with $n' \leq n_\omega$, is subsequently calculated as a function of L_i and s'.

With regard to the relative tillering rates that were discussed in the previous paragraphs, tiller population during the tillering phase is calculated with the following discrete differential equation.

$$n_{pop}(t+1) = n_{pop}(t) + \Delta n_{pop} \tag{4.2.3}$$

where

$$\Delta n_{pop} = n' \times n_{pop}(t) \tag{4.2.4}$$

and

$$n' = f(L_i, s') \leq n_{\omega} \tag{4.2.5}$$

and t is thermal time (HU_{16} in $°C \times d$).

4.2.6. The tiller senescence phase

Under normal high-density crop conditions, a characteristic phase of tiller senescence normally follows the tillering phase. Van Dillewijn (1952: 87) and Kanwar and Sharma (1974) noted that this phase is mainly driven by light competition in which younger, less competitive tillers would die due to the lack of sunlight. Unpublished results from J. Glover (SASA Experiment Station, Mt. Edgecombe, 1973) show that 75% of tillers that undergo senescence would die before they reach a height of $30cm$. Inman-Bamber (1994b) noted that younger tillers would die rapidly when 70% of PAR is intercepted by green foliage. This increase in senescence rate was found to be explicit and reasonably similar between cultivars and it was concluded that it could be interpreted as a predictable phenological stage in sugarcane crops.

For this model, tiller senescence was assumed to be driven by the availability of light to the individual tiller, which is expressed by LAI and s'. This phase continues until harvest and initiates when the youngest tiller in the crop has a leaf area (LA in cm^2) that is lower than a calculated minimum sustainable leaf area per tiller (LA'_{min} in cm^2), expressed in terms of LAI

4.2.6.1. THE CALCULATION OF LEAF AREA PER TILLER

It was assumed that no more than 12 leaves per tiller could be alive at any time. The green leaf area per tiller (LA in cm^2) could therefore be calculated by accumulating the values of $A_{max(j)}$ (eq. 3.2.5).

$$LA = \sum_{j=j'}^{n_{leaf}} A_{max(j)} \tag{4.2.6}$$

where n_{leaf} is the total number of leaves for the tiller and j' is the chronological number of the oldest green leaf.

The calculation in eq. 4.2.6 did not include the development of the youngest four leaves, which might not have reached their maximum potential areas yet. Although it could be addressed by incorporating leaf growth (eq. 3.2.4), it was not included for this study and all leaves were assumed to reach maximum potential leaf area within a short time. Since LA in eq. 4.2.6 would have discrete values, a logistical curve was fitted to implement a continuous function for this variable. This relationship is illustrated in Figure 4.4.

$$LA = \frac{4619.8}{1 + e^{0.31(13.5 - n_{leaf})}} \tag{4.2.7}$$

By using eq. 3.2.3 to calculate n_{leaf}, eq 4.2.7 introduces a simple method to calculate LA from HU_{10}.

4.3. Data and data derivation

Data from an irrigated experiment at La Mercy (*29°37' S, 31°8' E, elev. 115m*), reported by Singels *et al.* (1998), were used for this study. Two of five treatments that were replicated five times on $8 \times 10m$ plots were selected for analysis.

Treatment 1: Apply irrigation when the CANEGRO model indicates the soil water content (θ) to be below a certain value.

Treatment 2: Apply irrigation when the CANEGRO model indicates that the plant extractable soil moisture is lower than two times the atmospheric evaporative demand (E_T).

The experiment comprised of one plant crop and three consecutive ratoon crops over the period September 1994 to November 1998. Tiller numbers (n_{pop}) were recorded two to three weeks apart. Fractional *PAR* interception readings, using a ceptometer (Decagon Devices Inc.), were also made at similar intervals during the 2nd and 3rd ratoons. Daily minimum and maximum temperature, rainfall, humidity and solar radiation were available from nearby manual and automatic meteorological stations and a rain gauge. The plant crop, 1st and 2nd ratoons were used for model calibration while data from the 3rd ratoon were reserved for validation. The daily weather records, irrigation records and a representative soil profile (Singels *et al.*, 1998) were used to simulate the treatments with the CANEGRO model. These model outcomes show that both treatments had very little or no water stress during the plant, 1st and 2nd ratoons.

4.3.1. Tiller population

Due to the model's differential characteristics during the tillering and tiller senescence phases, daily population estimates were required for calibration purposes. The use of relative tillering rates per HU_{16} during the tillering phase (n_ω and n') also required continuous differentiable

population functions. Daily population estimates were subsequently obtained by fitting polynomial functions in terms of thermal crop age (ΣHU_{16}) to the experiment's observations.

$$n_{pop} = a_0 + a_1\Sigma HU_{16} + a_2\Sigma HU_{16}^2 + \ldots + a_5\Sigma HU_{16}^5 \qquad (4.3.1)$$

Figure 4.2 displays the tiller population observations and the fitted functions while Table 4.1 reflects the intervals and coefficients that were used in eq. 4.3.1.

Table 4.1. Intervals and coefficients for polynomial functions that were fitted to tiller population observations.

TREATMENT 1

	Interval ΣHU_{16}	a_0	a_1	a_2	a_3	a_4	a_5
Plant crop	151 – 930	-8.70×10^{4}	1.30×10^{3}	-7.22	1.95×10^{-2}	-2.07×10^{-5}	7.48×10^{-9}
	930 – 1500	-9.94×10^{6}	5.28×10^{4}	-1.05×10^{2}	1.02×10^{-1}	-4.82×10^{-5}	8.89×10^{-9}
1st Ratoon	100 – 530	-1.14×10^{6}	1.89×10^{4}	-9.18×10^{1}	2.10×10^{-1}	-2.22×10^{-4}	8.79×10^{-8}
	530 – 1240	-2.69×10^{6}	1.85×10^{4}	-4.22×10^{1}	4.71×10^{-2}	-2.63×10^{-5}	5.91×10^{-9}
2nd Ratoon	111 – 730	-5.97×10^{5}	8.43×10^{3}	-3.09×10^{1}	5.49×10^{-2}	-4.55×10^{-5}	1.40×10^{-8}
	730 – 1570	-1.70×10^{6}	6.12×10^{3}	-3.16	-4.48×10^{-3}	4.78×10^{-6}	-1.22×10^{-9}

TREATMENT 2

	Interval ΣHU_{16}	a_0	a_1	a_2	a_3	a_4	a_5
Plant crop	151 – 930	-2.58×10^{5}	3.57×10^{3}	-1.72×10^{1}	3.79×10^{-2}	-3.61×10^{-5}	1.23×10^{-8}
	930 – 1500	4.16×10^{6}	-1.51×10^{4}	2.18×10^{1}	-1.40×10^{-2}	3.56×10^{-6}	-1.40×10^{-10}
1st Ratoon	100 – 530	-9.25×10^{5}	1.52×10^{4}	-7.19×10^{1}	1.61×10^{-1}	-1.70×10^{-4}	6.70×10^{-8}
	530 – 1240	4.31×10^{4}	1.38×10^{3}	-1.41	-3.13×10^{-4}	6.77×10^{-7}	-1.32×10^{-10}
2nd Ratoon	111 – 730	-7.34×10^{5}	1.04×10^{4}	-3.89×10^{1}	7.12×10^{-2}	-6.20×10^{-5}	2.03×10^{-8}
	730 – 1570	1.30×10^{6}	-7.80×10^{3}	2.26×10^{1}	-2.79×10^{-2}	1.53×10^{-5}	-3.07×10^{-9}

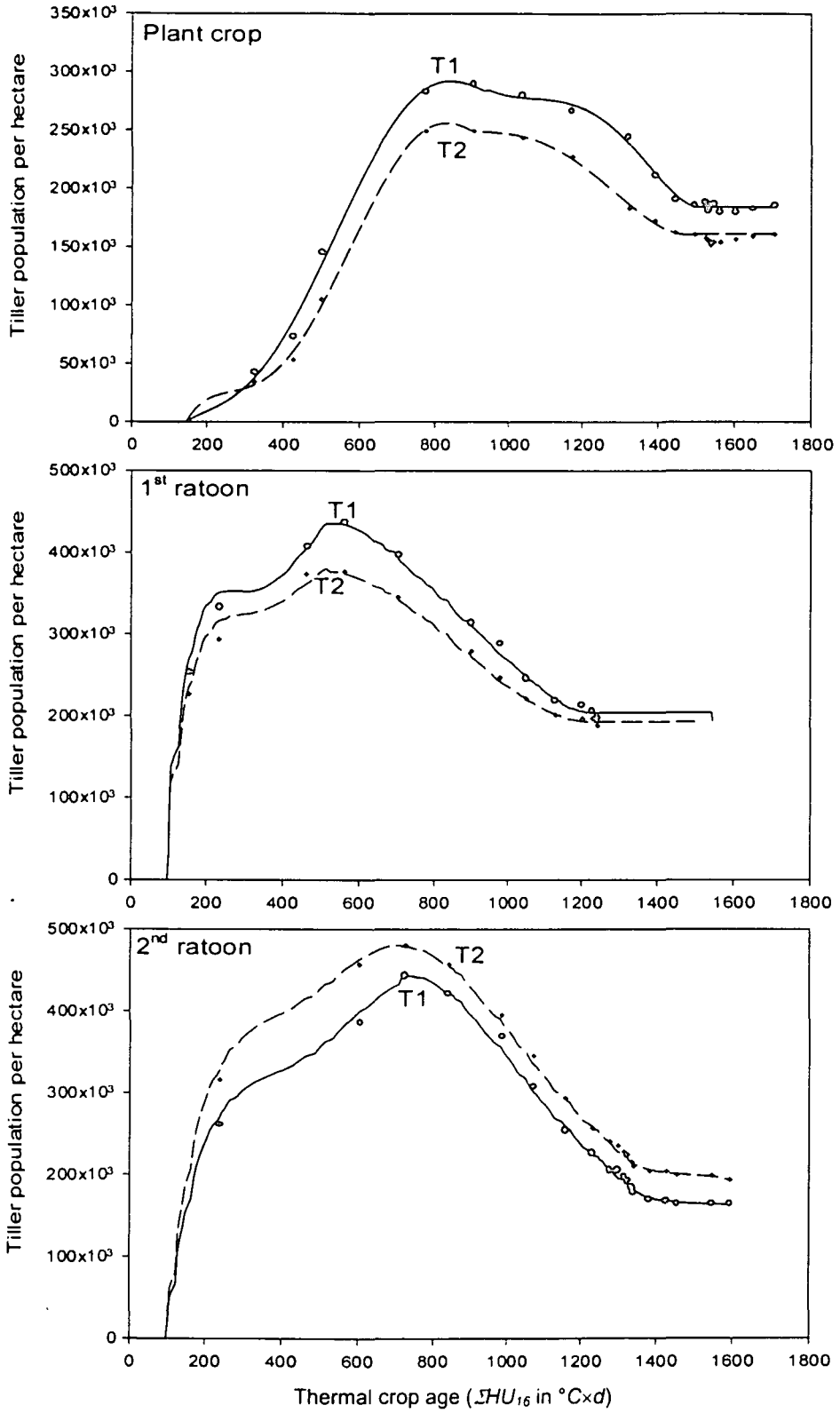

Figure 4.2. Tiller population for treatment 1 (T1) and treatment 2 (T2) from the La Mercy irrigation experiment. The solid lines are polynomial functions that were used to interpolate between observations.

4.3.2. Leaf area per tiller

The tiller senescence phase is based on the use of a minimum sustainable leaf area per tiller (LA'_{min}), it was therefore necessary to have estimates of LA for all the tillers. A statistical approach was followed to represent the distribution in LA among tillers at a specific time in the crop. This was done by firstly deriving distribution parameters for tiller age (ΣHU_{10}), then convert the age distribution parameters to n_{leaf} by using eq. 3.2.3 and then convert the n_{leaf} distribution parameters to LA by using eq. 4.2.7.

The daily population estimates that were derived in 4.3.1 were used to calculate daily crop estimates for the mean tiller age ($\overline{AGE}$), the variance in tiller age (σ_{AGE}^2) and the minimum and maximum tiller ages. It was assumed that during the tiller senescence phase, younger tillers would die first, implying a last in first out basis. Figure 4.3 illustrates these four age distribution parameters as calculated over the life span of the 1st treatment's 1st ratoon crop.

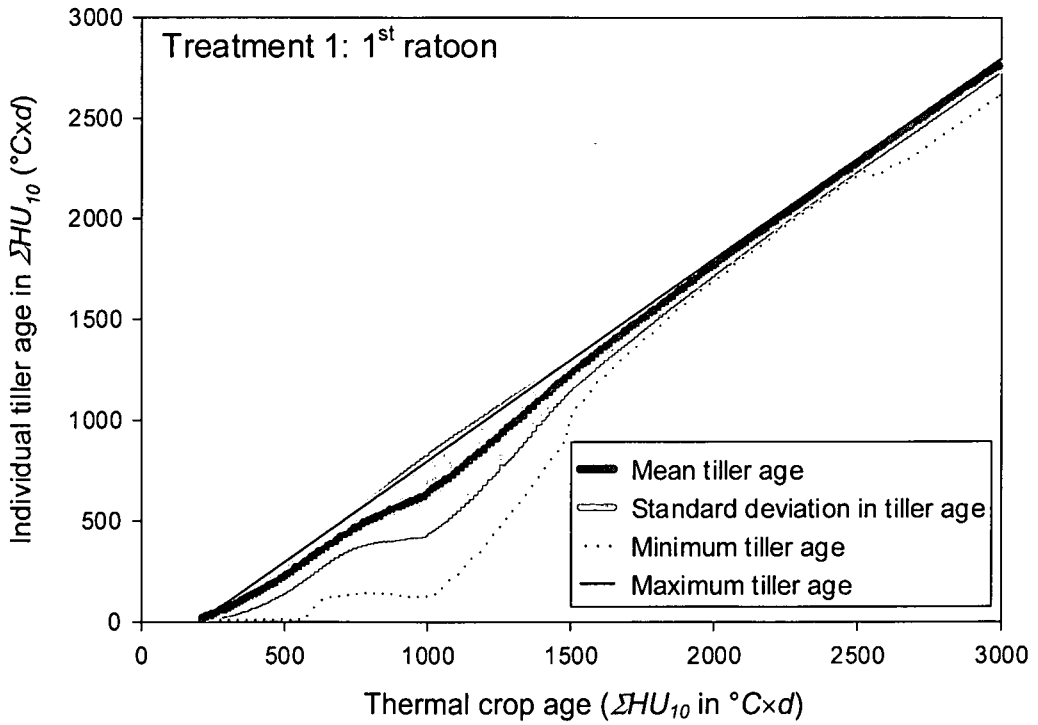

Figure 4.3. Mean tiller age (solid black line), the standard deviation in tiller age (gray shaded) and maximum and minimum tiller ages (thin solid and dotted lines respectively) plotted against the thermal age of the crop.

By making use of eq. 3.2.3 and the age distribution parameters that were calculated in the previous paragraph, the mean, minimum and maximum number of leaves per tiller ($\overline{n_{leaf}}$, $n_{minleaf}$ and $n_{maxleaf}$) at a given time in the crop could be calculated. The variance in leaf number per tiller (σ_{nleaf}^2) was linearly converted from the variance in tiller age (Rice 1995: 123). This was done by taking the pro-rata contribution of the two slopes in eq. 3.2.3 (ξ_1^{-1} and ξ_2^{-1}) after assuming that the data was closely symmetrically distributed.

$$\sigma_{nleaf}^2 = p_1 \frac{1}{\xi_1^2} \sigma_{AGE}^2 + p_2 \frac{1}{\xi_2^2} \sigma_{AGE}^2 \qquad (4.3.2)$$

where ξ_1 and ξ_2 are the first and second phyllochron intervals, σ_{AGE}^2 is the variation in tiller age and p_1 and p_2 ($p_1+p_2=1$) are the proportions of the interval [$\overline{AGE}-\sigma_{AGE}$, $\overline{AGE}+\sigma_{AGE}$] that are respectively smaller and greater than $14\xi_1$.

By using $\overline{n_{leaf}}$, $n_{minleaf}$ and $n_{maxleaf}$ in eq. 4.2.7, the mean, minimum and maximum leaf area per tiller ($\overline{LA}$, LA_{min} and LA_{max} in cm^2) could be calculated. The variance in leaf area over tillers (σ_{LA}^2) was derived in a similar fashion to σ_{nleaf}^2. Since σ_{nleaf}^2 was small for all crops ($\sigma_{nleaf}<3.1$), a simplified method was used to calculate σ_{LA}^2. Two separate linear conversions according to Rice (1995: 123) for the intervals [$\overline{n_{leaf}}-\sigma_{nleaf}$, $\overline{n_{leaf}}$] and [$\overline{n_{leaf}}$, $\overline{n_{leaf}}+\sigma_{nleaf}$] were used. The dotted lines in Figure 4.4 illustrate for example where σ_{nleaf} had a value of 3.0. The range [$\overline{n_{leaf}}-\sigma_{nleaf}$, $\overline{n_{leaf}}+\sigma_{nleaf}$] was subdivided into two equal ranges with separate linear slopes (b_1 and b_2).

$$\sigma_{LA}^2 = 0.5b_1^2\sigma_{nleaf}^2 + 0.5b_2^2\sigma_{nleaf}^2 \qquad (4.3.3)$$

where b_1 and b_2 were calculated by making use of the function $LA(x)$ (eq. 4.2.7),

$$b_1 = \frac{LA\left(\overline{n_{leaf}}\right) - LA\left(\overline{n_{leaf}} - \sigma_{nleaf}\right)}{\sigma_{nleaf}} \qquad (4.3.4a)$$

$$b_2 = \frac{LA\left(\overline{n_{leaf}} + \sigma_{nleaf}\right) - LA\left(\overline{n_{leaf}}\right)}{\sigma_{nleaf}} \qquad (4.3.4b)$$

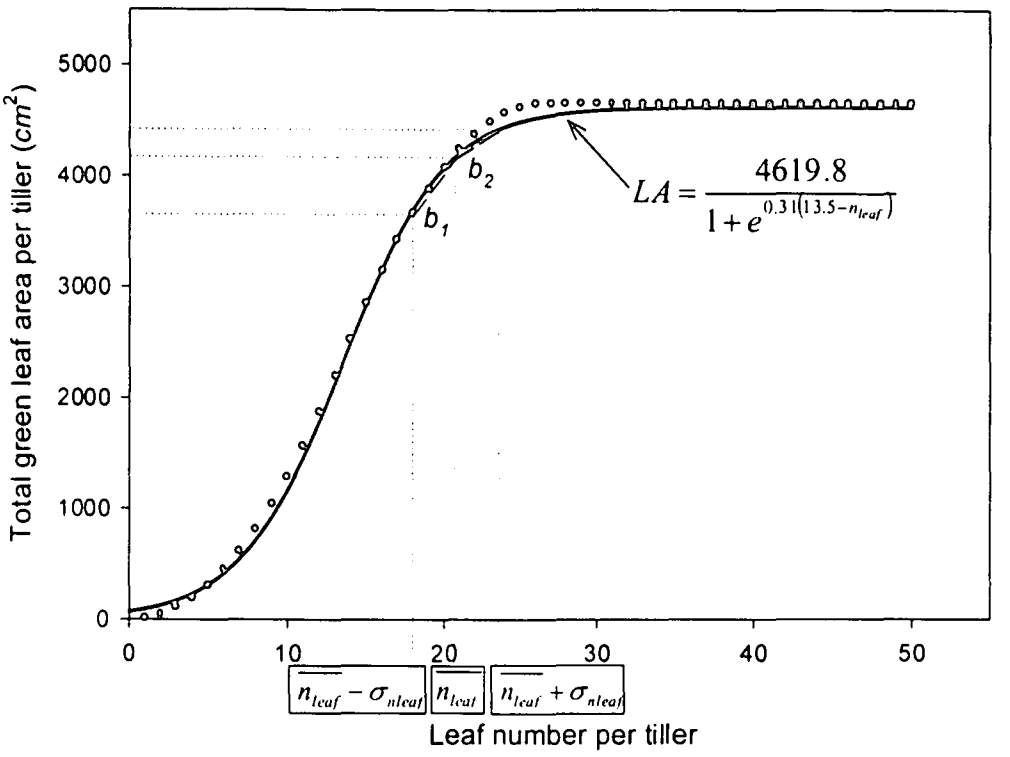

Figure 4.4. The logistical function that was used to estimate leaf area per tiller (solid black line). The black circles are the calculated *LA* values according to eq. 4.2.6. The dotted lines indicate how the crop's variation in leaf number was converted to variation in leaf area by simplifying the trend with two linear conversions (b_1 and b_2).

After initial investigations it was assumed that the distribution for *LA* during the senescence phase could be represented by a beta distribution function, $f(x)$ (Rice, 1995: 593-597) with $LA \in [0.9 \times LA_{min}, 1.1 \times LA_{max}]$.

$$f(x) = \frac{\Gamma(p+q)}{\Gamma(p)\Gamma(q)} x^{p-1}(1-x)^{q-1} \qquad (4.3.5)$$

where Γ is the gamma function (Rice, 1995: 50-53), p and q are distribution parameters and x ($cm^2 \times cm^{-2}$) is a normalised leaf area per tiller value that ranges from 0 to 1;

$$x = \frac{LA - 0.9LA_{min}}{1.1LA_{max} - 0.9LA_{min}} \qquad (4.3.6)$$

After Essenwanger (1976: 42-44) it is known that a beta distribution function falling in the range $LA \in [0.9 \times LA_{min},\ 1.1 \times LA_{max}]$ will have a mean ($\overline{LA}$) and variance ($\sigma_{LA}^{\ 2}$) according to the following equations:

$$\overline{LA} = 0.9LA_{min} + \frac{(1.1LA_{max} - 0.9LA_{min})p}{p+q} \tag{4.3.7}$$

$$\sigma_{LA}^{\ 2} = \frac{(1.1LA_{max} - 0.9LA_{min})^2 pq}{(p+q)^2(p+q+1)} \tag{4.3.8}$$

By using substitution, eqs. 4.3.6, 4.3.7 and 4.3.8 could be used to find solutions for p and q. The determination of these solutions are listed in more detail in Appendix B.

$$p = \frac{-\bar{x}\sigma^2 + \bar{x}^2 - \bar{x}^3}{\sigma^2} \tag{4.3.9}$$

and

$$q = \frac{p}{x} - p \tag{4.3.10}$$

where

$$\sigma^2 = \frac{\sigma_{LA}^{\ 2}}{(1.1LA_{\max} - 0.9LA_{\min})^2} \tag{4.3.11}$$

The above derived p and q values followed similar trends for all ratoon crops and q could be expressed in terms of LA_{max}, while p followed a non-linear relationship to q. Eqs. 4.3.12 and 4.3.13 were subsequently used to estimate likelihood values for p and q.

$$q = \begin{cases} -0.1291 + 4.025 \times 10^{-4} LA_{max} + 6.184 \times 10^{-8} LA_{max}^{\ 2} & \mid LA_{max} \le 2500 \\ 1.424 - 9.362 \times 10^{-5}(LA_{max} - 2500) & \mid LA_{max} > 2500 \end{cases} \tag{4.3.12}$$

$$p = -8.556 \times 10^{-3} + 1.257q - 0.2572q^2 \tag{4.3.13}$$

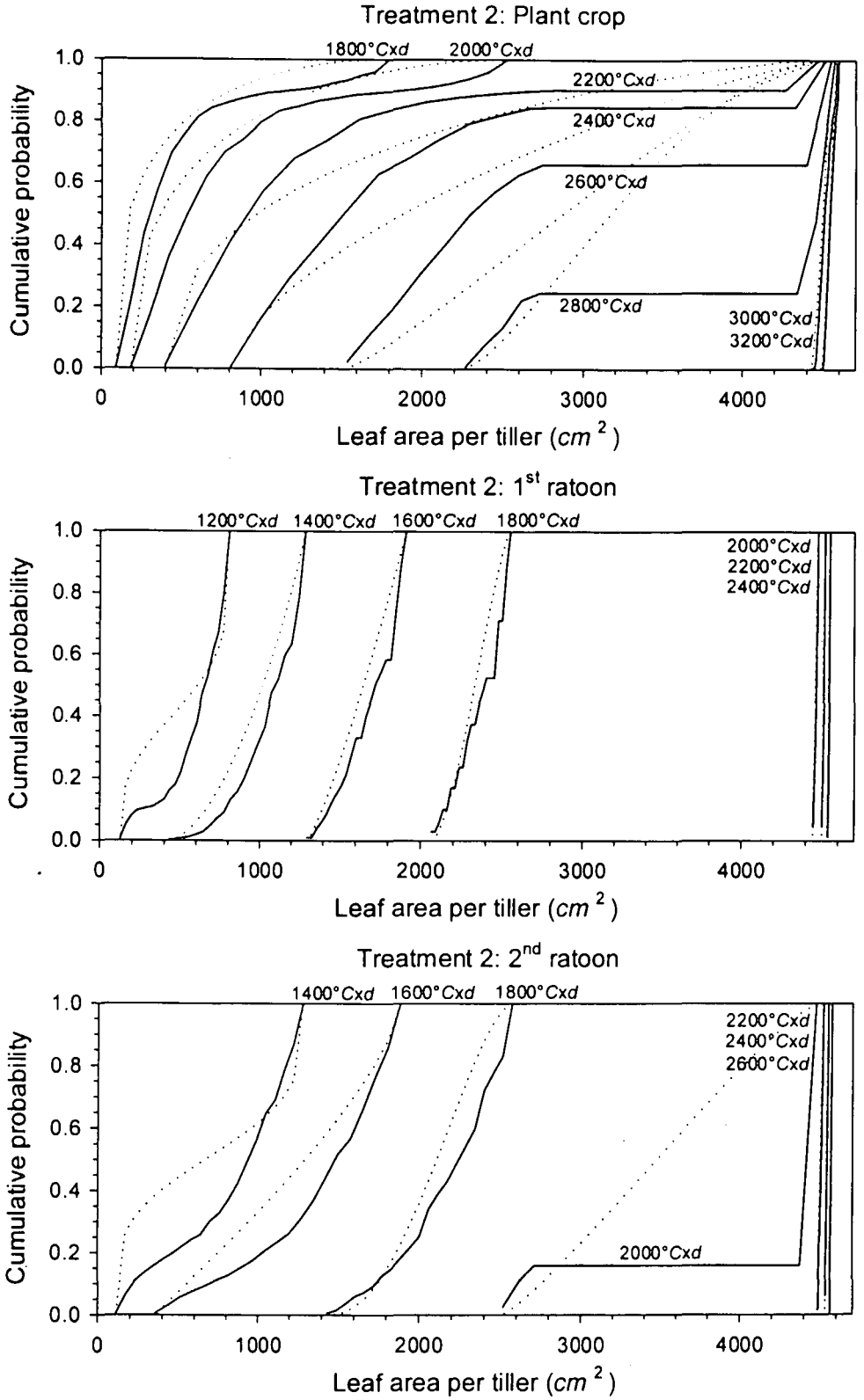

Figure 4.5. Cumulative distribution in *LA* (solid lines) and the beta distribution (dotted lines) during different times of the senescence phase of the (a) plant crop, (b) 1st ratoon and (c) 2nd ratoon for treatment 2.

A goodness of fit test was done after every 200°C×d (ΣHU_{10}) by calculating each individual tiller's leaf area and comparing this distribution of LA with the corresponding beta distribution. The conventional Pearson's χ^2 test (Rice, 1995: 241-243) was used to assess the similarity between the two distributions. Results from the χ^2 test did not support the beta distribution function with confidence. A possible reason for this could be the origin of the data. Large artificially generated samples from the approximated population polynomial functions (4.3.1) were used. The suitability of this data in the Pearson's χ^2 test can be questioned. Cumulative distributions of both the calculated LA and the beta function were subsequently plotted after every 200°C×d (ΣHU_{10}). Figures 4.5(a,b,c) illustrate these distribution functions for the plant crop, 1st ratoon and 2nd ratoon for treatment 2.

Form Figures 4.5(a,b,c) it is evident that the beta distribution function often deviates from the distribution of the calculated LA values. The fact that LA was calculated with deterministic equations after fitting polynomial functions to population counts adds to the uncertainty of these distributions. It is probable that accurate LA measurements, which were not available for this study, are necessary to establish better distribution parameters.

From the population functions (eq. 4.3.1) it can be shown that the fraction of tillers that underwent senescence on a certain day was always less than 2% of the crop population. From Figure 4.5 it can be seen that no large deviations between the distribution of LA and the beta distribution exist below 0.02 and it was subsequently assumed that the beta distribution sufficiently represents LA to calibrate a tiller senescence component for this model.

4.3.3. Leaf area index and light interception

Leaf area index and light interception values were required for calibration purposes. Daily LAI values were used to determine a relationship with LA'_{min} and a continuous differentiable function for L_i, expressed in terms of HU_{16}, was used to determine a relationship with n'. By

making use of the population functions in 4.3.1 and $\overline{LA}$ as derived in 4.3.2, daily leaf area index and light interception values could be calculated from eq. 3.2.6 and eq. 3.2.8 respectively. Figure 4.6 illustrates the calculated L_i values plotted with the field observations that were done during the 2nd ratoon. Only the calculated values were used in further analysis.

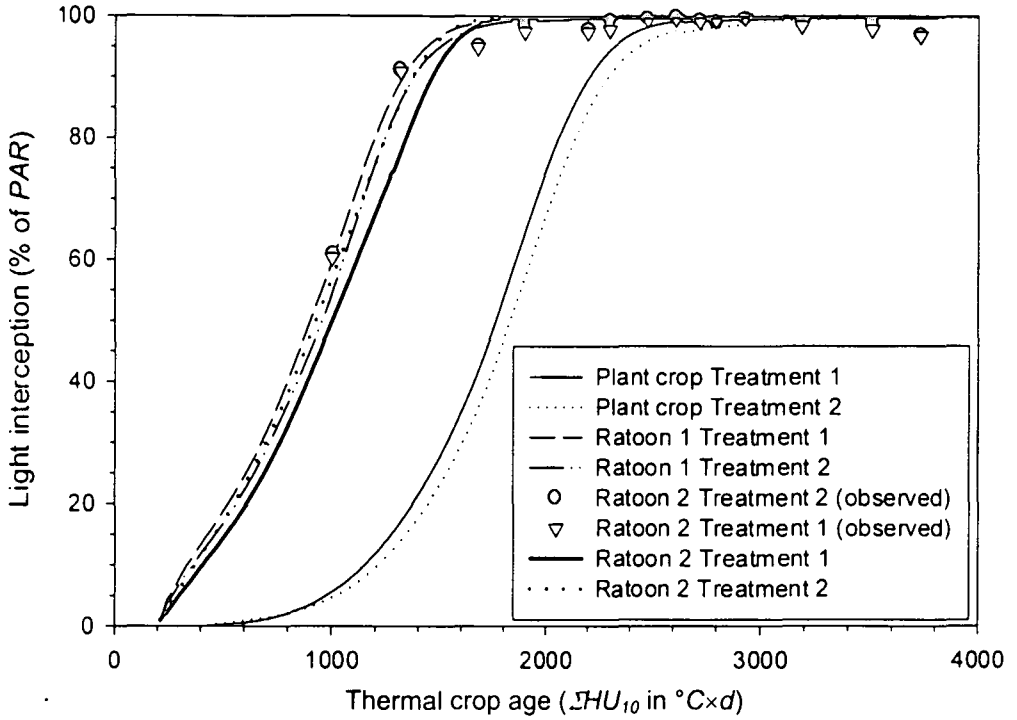

Figure 4.6. Light interception for treatment 1 and 2 for the plant crop and first two ratoons. Observed values of the second ratoon are indicated with symbols (∘, ∇).

Tillering was not expected to play a role once L_i>80%. Continuous differentiable functions were therefore fitted between L_i and ΣHU_{16} where $L_i \leq 80\%$. Values for L_i during plant crops could be represented by a logistic function, while ratoon crops were represented by linear functions. Table 4.2 shows the equations and coefficients that were used for these functions.

Table 4.2. Equations and the coefficients that were used to express L_i ≤80% in terms of ΣHU_{16}.

Equation used: $L_i = \frac{100}{1 + e^{-k_1((\Sigma HU_{16} - 146) - k_2)}}$	**Plant crop**	
Treatment 1:	k_1=0.00709 k_2=859.219	
Treatment 2:	k_1=0.00689 k_2=902.185	
Equation used: $L_i = k_0 + k_1 \Sigma HU_{16}$	**Ratoon 1**	**Ratoon 2**
Treatment 1:	k_0=-14.8521 k_1=0.14020	k_0=-16.8069 k_1=0.12039
Treatment 2:	k_0=-15.0822 k_1=0.13293	k_0=-16.8076 k_1=0.13116

4.4. Model calibration

4.4.1. The telomechron interval

Due to fewer initial buds in the soil, population numbers of the plant crop increased slower. This prolonged the time for primary tillers to undergo tillering under low L_i values. Since low L_i values suggest less light competition, the starting period of the plant crop was selected to determine the telomechron interval and the integral of eq. 4.2.2 was fitted to the first three data points of both treatments.

The telomechron interval was found to be of 128.6 and 141.1°C×d for treatments 1 and 2 respectively. A mean of 134.8°C×d was therefore assumed for this study. This interval equals a period of 24 days at a mean temperature of 21.6°C. It was less than half of the expected 6 to 7 phyllochron intervals (6.5×ξ_1) that would equal 61 days at the same mean temperature. The assumption of a single constant interval before any higher order tiller would emerge, could be an over simplification of the tillering process. These results suggest that shorter intervals might be expected for the emergence of tertiary or higher order tillers. It should be noted that

should be noted that only six data points were available for these analyses. The lack of more comprehensive observations restricted further refinements to the model at this stage.

4.4.2. The maximum relative tillering rate and stool diameter correction factor

From eq. 4.2.1 and the results in the previous paragraph it was calculated that the maximum relative tillering rate (n_ω) is $0.00742 tillers \times tiller^{-1} \times °C^{-1} \times d^{-1}$. By using eq. 4.3.1 and Table 4.2 the functions f_1 and f_2 were used to represent n_{pop} and L_i respectively. These functions are continuous and have continuous derivatives during the tillering phase.

$$n_{pop} = f_1(\Sigma HU_{16}) \tag{4.4.1}$$

$$L_i = f_2(\Sigma HU_{16}) \tag{4.4.2}$$

With n_{peak} representing the peak of each population curve, n_{pop} could be normalised to range between 0 and 1 by dividing f_1 with n_{peak}. By substituting ΣHU_{16} in f_1 with the inverse function of f_2, the normalised population (n'_{pop} expressed as a fraction of n_{peak}) could be expressed in terms of L_i (eq. 4.4.3). Figure 4.7 illustrates the results from eq. 4.4.3 for the tillering phase where n'_{pop} is expressed in terms of L_i.

$$n'_{pop} = \frac{f_1\left(f_2^{-1}(L_i)\right)}{n_{peak}} \tag{4.4.3}$$

The results from eq. 4.4.3, as seen in Figure 4.7, shows distinctly different responses between the plant, 1st ratoon and 2nd ratoon crops. These differences were used to calibrate the stool diameter correction factor (s'). The mean normalised population increment per unit light interception for the range $n'_{pop} \in [40\%, 100\%]$, expressed in (% of n_{peak})×(% of PAR)$^{-1}$, was calculated. This slope (s) decreased over ratoon numbers. Values for s for individual crops are reflected in Table 4.3.

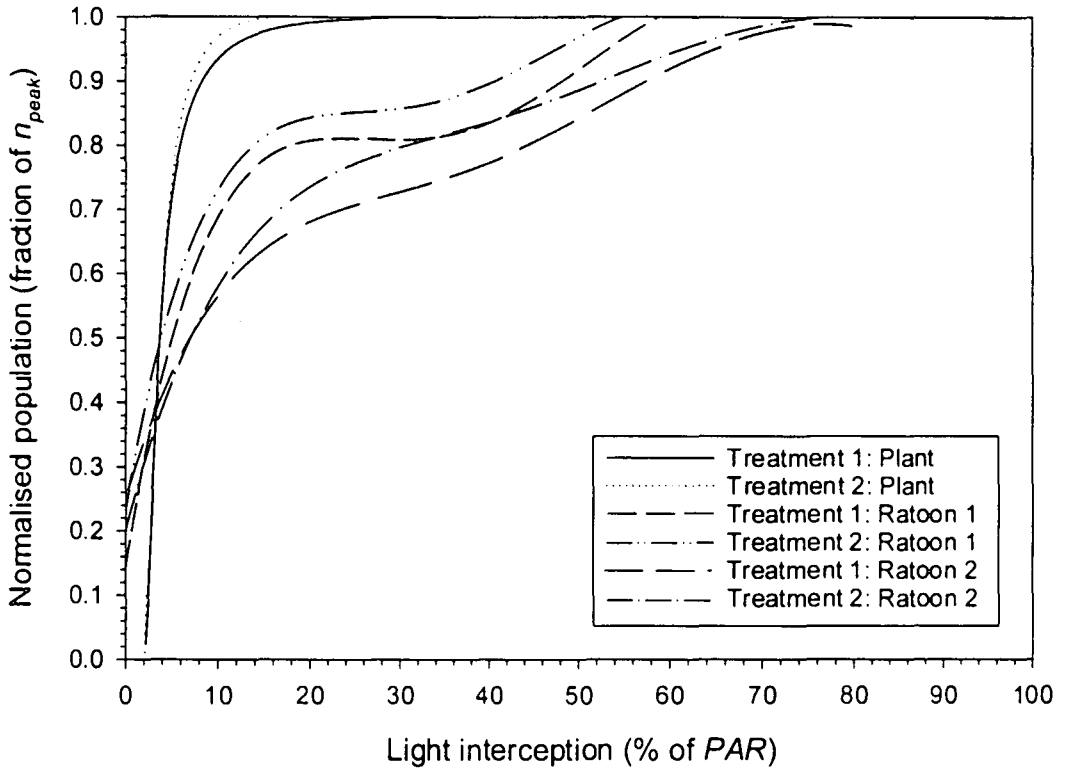

Figure 4.7. Normalised population curves for each treatment plotted against the corresponding light interception.

Table 4.3. Mean slope between $n'_{pop} \in [40\%, 100\%]$ and L_i for different treatments and ratoons. Values are expressed in $\%\times\%^{-1}$.

Ratoon	Treatment 1	Treatment 2	Mean
0	6.6667	3.2787	4.9727
1	1.2552	1.1561	1.2056
2	0.9023	0.9023	0.9023

Further analysis on the results in Table 4.3 suggested that s follows a logarithmic trend with an asymptote at $0.87\%\times\%^{-1}$ (Figure 4.8). This made it possible to calculate the stool diameter correction factor (s') as follows:

$$s' = \frac{s}{0.87} \tag{4.4.4}$$

where

$$s = 100 \times e^{-2.3754 \times ratoon - 3.3021} + 0.87 \tag{4.4.5}$$

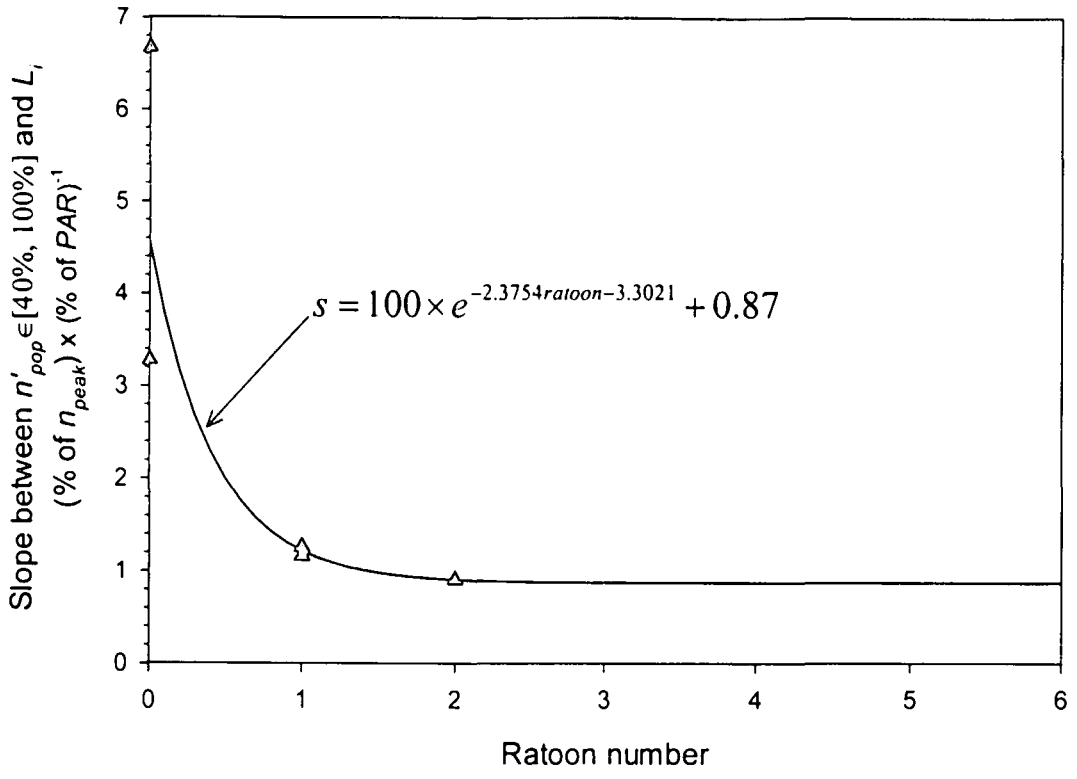

Figure 4.8. The relationship between s and ratoon number. Symbols (△) are the individual values for each crop.

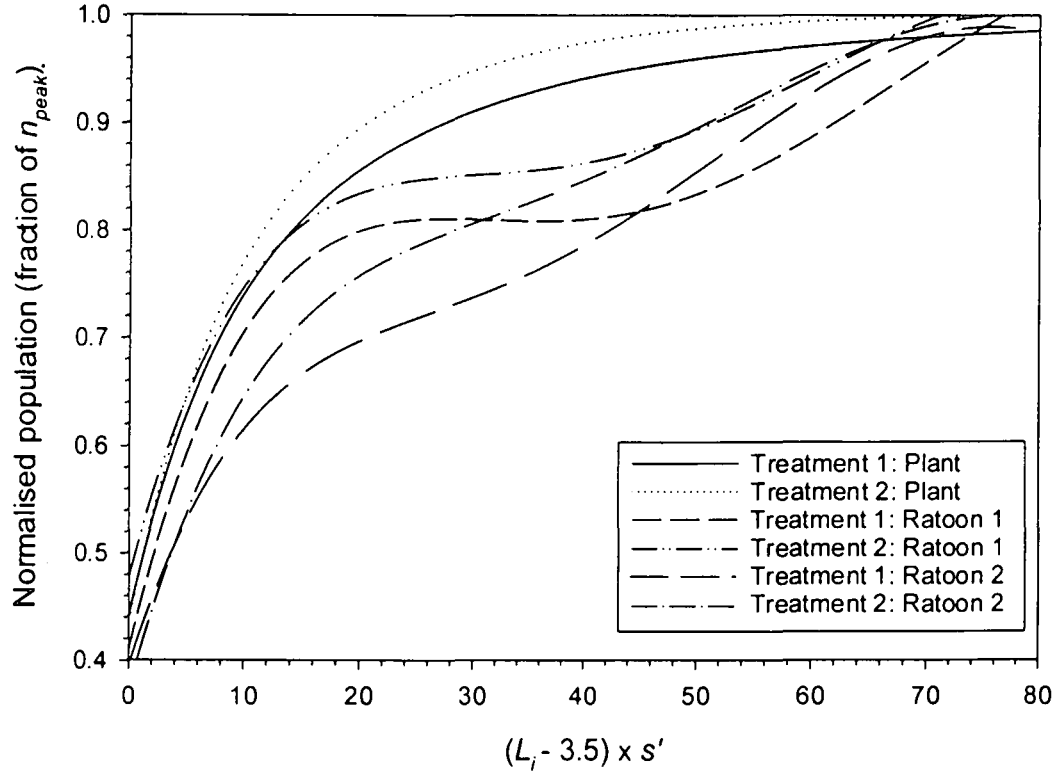

Figure 4.9. Normalised population curves drawn against light interception after a stool diameter correction was made.

4.4.3. Relative tillering rate under competitive conditions

In order to implement the stool diameter correction factor, the results of eq. 4.4.3 was plotted against $s' \times (L_i - 3.5)$. Figure 4.9 reflects these corrected values and shows a significant improvement over the results of Figure 4.7.

Through the differentiation of eq. 4.4.3, the relative tillering rate under light competitive conditions (n' in $tillers \times tiller^{-1} \times °C^{-1} \times d^{-1}$) could now be determined and be expressed in terms of the corrected light interception ($s' \times (L_i - 3.5)$).

$$n' = \frac{\frac{df_1}{d\Sigma HU_{16}} \times n_{peak}^{-1}}{f_1 \times n_{peak}^{-1}} = \frac{\frac{df_1}{d\Sigma HU_{16}}}{f_1} \qquad (4.4.6)$$

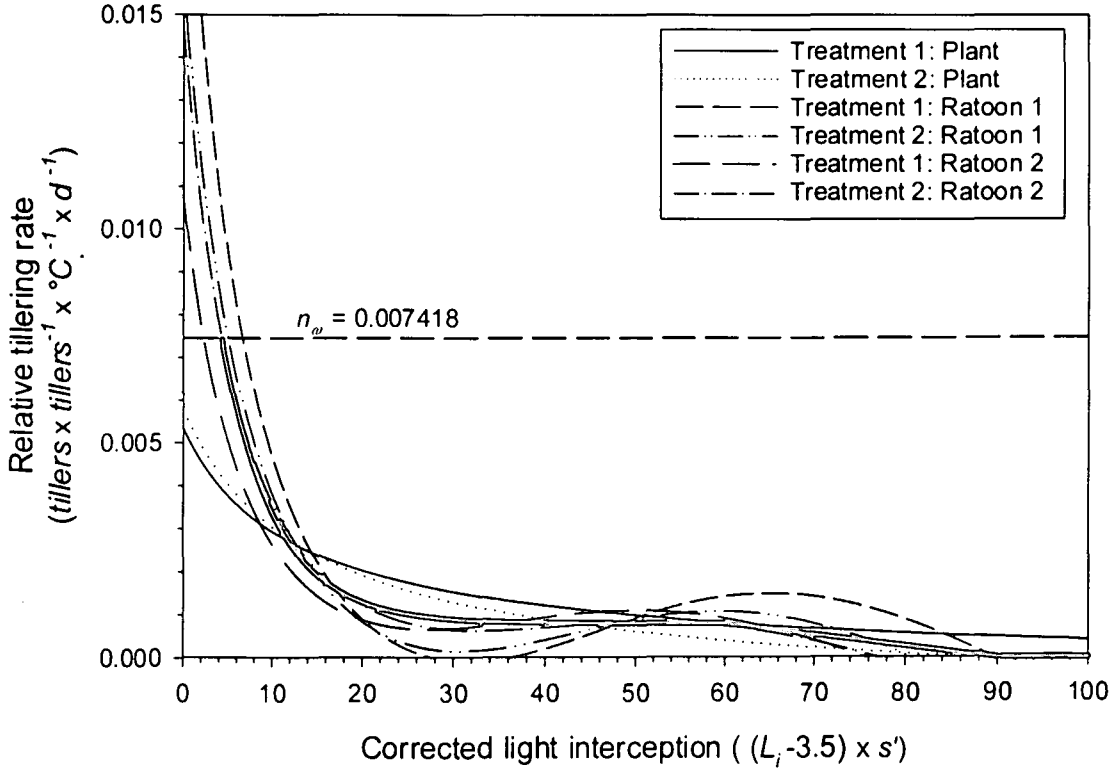

Figure 4.10. Relative tillering rates drawn against the stool diameter corrected light interception. The thick solid line is a fitted function to represent this trend.

Figure 4.10 illustrates n' drawn against $s' \times L_i$. This trend could be represented by eq. 4.4.7 (thick black line). The dashed horizontal line is n_∞, which is the maximum relative tillering

rate that can occur. Differences between curves from different ratoons and treatments could be based on the polynomial functions that were used to estimate tiller population (eq. 4.3.1).

$$n' = \begin{cases} \dfrac{0.01346}{e^{0.16511 \times s' \times (L_i - 3.5)}} + 0.0008 & \mid (s' \times (L_i - 3.5)) \leq 60 \\ 0.0008 - 2.667 \times 10^{-5} \times \left((s' \times (L_i - 3.5)) - \left(\dfrac{60}{s'} + 3.5 \right) \right) & \mid (s' \times (L_i - 3.5)) > 60 \end{cases} \tag{4.4.7}$$

4.4.4. Primary tiller emergence and initial number of buds

It was assumed that all tillers that emerged at higher relative rates than n_ω (Figure 4.10) were primary tillers. It was also assumed that the primary tiller emergence phase ended at the stage when a relative emergence rate of n_ω was reached.

$$n_{popi} = f_1 \tag{4.4.8}$$

where f_1 specifically satisfies

$$n_\omega = \frac{\dfrac{df_1}{d\Sigma HU_{16}}}{f_1} \tag{4.4.9}$$

The above calculation provided estimates for n_{popi} and the corresponding L_i and thermal crop ages (ΣHU_{16} and ΣHU_{10}) at which the primary tiller emergence phase terminated. Insufficient data existed to derive any of these values for the two planted crops. Table 4.4 reflects these values of n_{popi}, L_i, ΣHU_{16} and ΣHU_{10} for all the ratoon crops. The observed tiller population at the harvest of the previous ratoon of each crop was also included in Table 4.4.

Results from Table 4.4 suggest that a mean ratio of 1.621 new primary tillers per harvested tiller in the previous ratoon would emerge. By assuming that buds were $10cm$ below the surface, $203°C \times d$ (HU_{10}) would have lapsed during the pre-germination and pre-emergence phases. Results from Table 4.4 suggest that the primary tiller emergence phase is terminated

at a thermal crop age of 356.4°C×d (HU_{10}), which therefore will assume a fixed duration of 153.4°C×d (HU_{10}) for the primary tiller emergence phase.

Table 4.4. Number of primary tillers in each crop and the specific L_i, ΣHU_{10} and ΣHU_{16} values where all primary tillers have emerged above the ground. The mature tiller population of the previous ratoon and its ratio to n_{popi} are reflected in the last two columns. Due to insufficient data, no values could be derived for the plant crops.

Crop and Treatment	L_i (%)	ΣHU_{10} (°C×d)	ΣHU_{16} (°C×d)	n_{popi} ($tillers \times ha^{-1}$)	***Previous ratoon*** ($tillers \times ha^{-1}$)	***Ratio***
Treatment 1: Ratoon 1	8.4	345.65	165.847	278277	150000	1.855
Treatment 2: Ratoon 1	7.2	349.40	167.624	246170	156000	1.578
Treatment 1: Ratoon 2	5.8	365.25	187.766	206591	145000	1.425
Treatment 2: Ratoon 2	7.8	365.20	187.61	250407	154000	1.626
Mean	7.3	356.38	177.21	245361	151250	1.621

4.4.5. Tiller senescence

Tiller senescence was based on the inability of a tiller to sustain itself under competitive conditions. The leaf area per tiller (LA) was considered to be a measure of tiller sustainability under competitive light conditions. Tillers with less than a minimum sustainable leaf area (LA'_{min} in cm^2) would die. The daily fraction of tiller senescence was derived from the population polynomial functions (eq. 4.3.1). By making use of the inverse of the beta function (eq. 4.4.10), the daily tiller senescence fraction could be converted to the corresponding LA value, which was assumed to be the minimum sustainable leaf area per tiller (LA'_{min} in cm^2) for that day.

$$\frac{LA'_{min} - LA_{min}}{LA_{max} - LA_{min}} = x' = f^{-1}(f_s, p, q) \qquad (4.4.10)$$

where x' is the normalised leaf area fraction (eq. 4.3.6) and f_s is the daily tiller senescence fraction.

The daily LA'_{min} values were expressed in terms of LAI and s'. Eq. 4.4.11 and Figure 4.11 reflect this relationship.

$$LA'_{\min} = e^{3.0476+0.6079(LAI+0.4s')} \qquad (4.4.11)$$

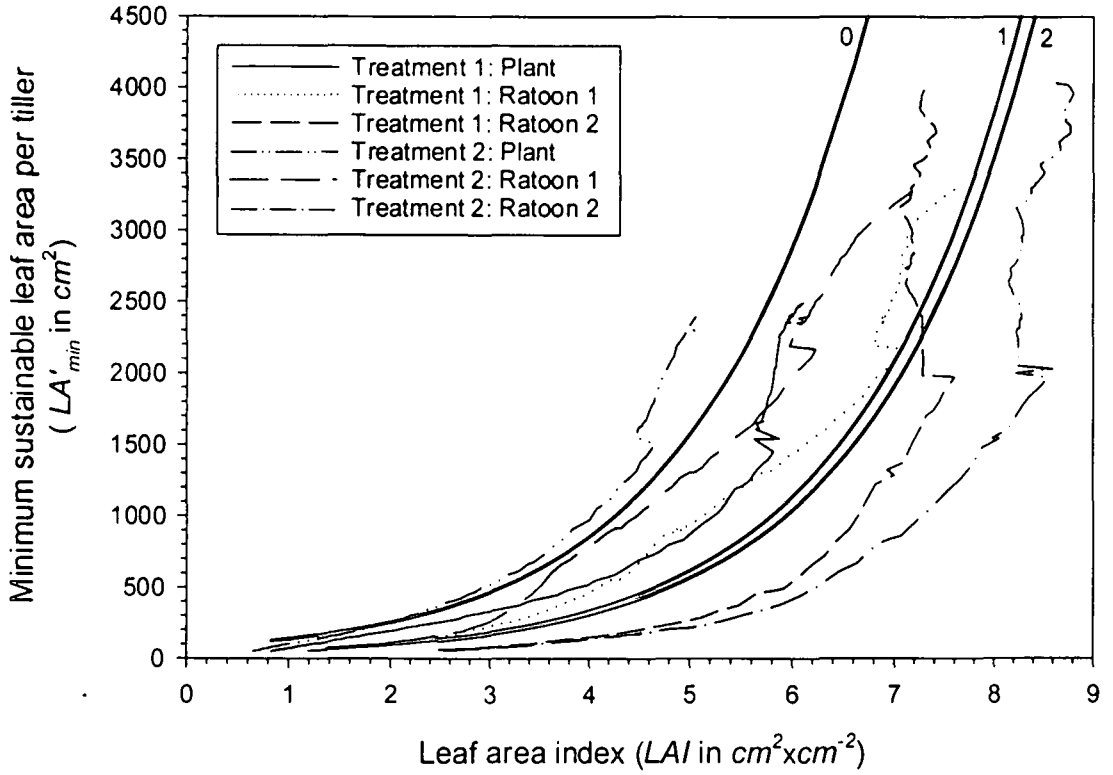

Figure 4.11. LA'_{min} drawn against LAI for the plant crop (0), 1st ratoon (1) and 2nd ratoon (2). The three solid lines represent the stool diameter dependant trend that was used to simulate this relationship.

4.5. Model assessment and validation

Outcomes from the proposed tiller model were validated against the independent 3rd ratoon's data for both treatments. This ratoon stretched over the period from 11 November 1997 to 10 November 1998. Treatment 1 was well irrigated and pre-simulated CANEGRO outcomes indicated minor water stress of less that 8 days during the course of this crop. Irrigation specifications for treatment 2 differed from previous ratoons and the CANEGRO model suggested that this treatment was exposed to more than 130 days water stress. Figures 4.12

and 4.13 illustrate the outcomes of the mechanistic tiller model for population and light interception with the corresponding CANEGRO outcomes and field observations.

The dormant period of $90°C\times d$ (ΣHU_{10}) suggests that germination started on 18 November 1997, 7 days after the crops were initiated. The length of the CANEGRO model's pre-emergence phase is determined by a model input, which was also assumed to be 7 days. The mature tiller population at the end of the 2nd ratoon for treatments 1 and 2 were 164000 and $171000 tillers\times ha^{-1}$ respectively. By using the ratio of 1.621, it was assumed that 265844 and $277191 tillers\times ha^{-1}$ primary tillers emerged for the two treatments in their 3rd ratoons. All primary tillers were expected to have emerged after $356°C\times d$ (ΣHU_{10}), which was on the 15th of December 1997, at the age of 34 days.

Secondary tillering started at a rate of 40% of n_ω ($0.00297 tillers\times tiller^{-1}\times °C^{-1}\times d^{-1}$). This was due to the large number of primary tillers, which caused L_i to have a value of 21.1% at the end of the primary tiller emergence stage, subsequently inflicting light competition. The stool diameter adjustment factor (s') was 1.0034 for the 3rd ratoon, which suggests that stools had reached their maximum diameters and could not be anticipated to expand much further. However, when compared with the observations the actual population peak (n_{peak}) was 30% higher than anticipated, suggesting more profuse tillering than what the model could simulate. Further research into this matter would be required to supply a sufficient explanation for this occurrence.

Tiller senescence started at a crop age of 79 days on the 28th of January for both treatments. Light interception on this day were 72% and 74% for treatments 1 and 2, respectively. LA'_{min} was initially too low to cause older tillers to undergo senescence, but restricted the development of new tillers. This caused a 30-day population plateau. Senescence of older tillers only occurred after 27 February, when the crop was 109 days old. Initial senescence

rates were high, but slowed down as remaining tillers became competitive enough to sustain themselves.

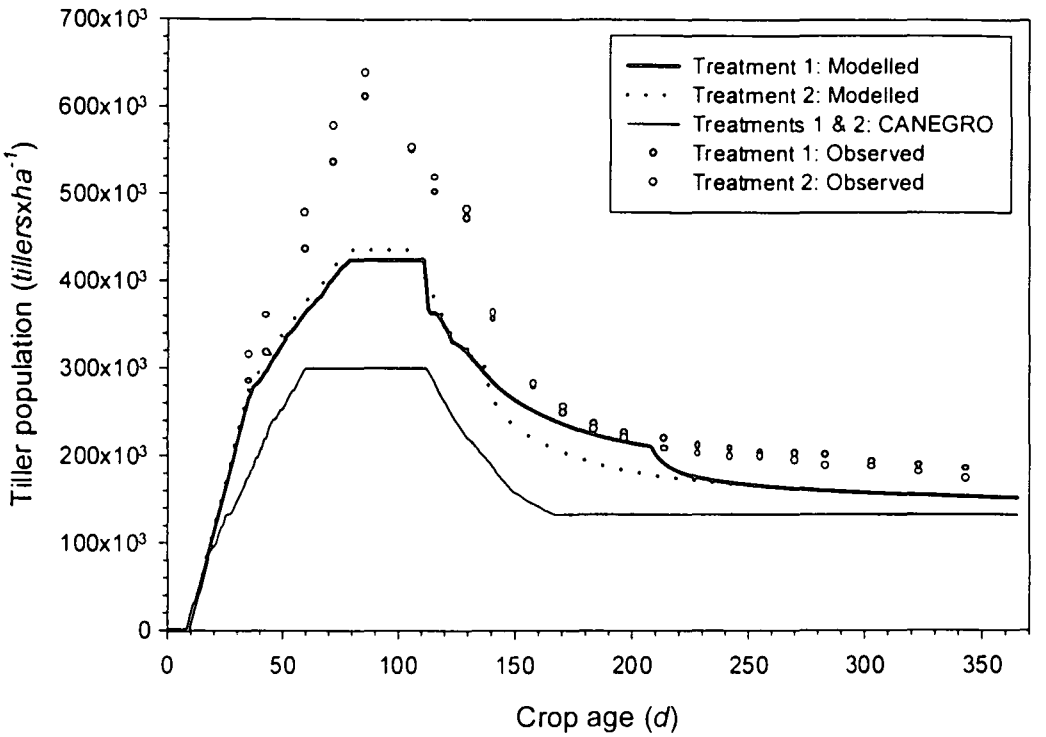

Figure 4.12. Simulated and observed tiller populations during the 3rd ratoon.

From Figure 4.13 it is evident that the mechanistic tiller model simulated light interception better than the CANEGRO model. Both models, however, still underestimated L_i, which was most likely caused by the models' inabilities to acurately simulate tiller numbers during the tillering phase. Although the CANEGRO model suggested that treatment 2 experienced more severe water stress, field observations of L_i carry little evidence to support this conjective. The mechanistic tiller model, which does not simulate water stress, still outperformed the CANEGRO model. This supports previous findings that the CANEGRO model simulates water stress too severely (van Antwerpen, 1998: 1).

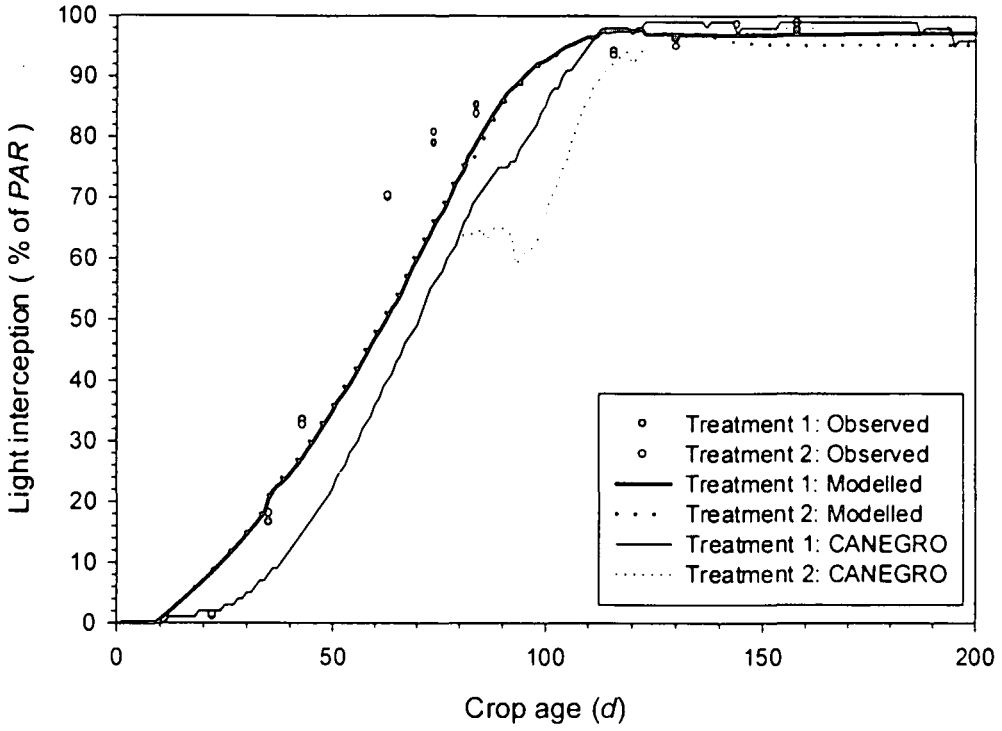

Figure 4.13. Simulated and observed light interception during the 3rd ratoon.

Tiller population and light interception measurements were formally assessed by calculating the maximum error (*ME*) and root mean square error (*RMSE*) (Mathews, 1987: 215) between observed (*O*) and estimated (*E*) values. Despite this data being serially correlated in time (with crop age) which reduces the independence of the data, these statistics are useful for comparative purposes. Table 4.5 shows these results.

$$ME = \max_{1 \le k \le N} \{|E_k - O_k|\} \tag{4.5.1}$$

$$RMSE = \sqrt{\frac{1}{N}\sum_{k=1}^{N}(E_k - O_k)^2} \tag{4.5.2}$$

where N is the number of observations.

Table 4.5. *ME* and *RMSE* values for both the CANEGRO model and the mechanistic tiller model.

		ME		*RMSE*	
		CANEGRO	**Tiller model**	**CANEGRO**	**Tiller model**
Population (*tillers×ha*$^{-1}$)	**Treatment 1**	310882	187056	149084	78577
	Treatment 2	338384	202971	160361	87538
Light interception (% of *PAR*)	**Treatment 1**	29.95	19.55	13.84	8.50
	Treatment 2	30.31	18.55	14.58	9.21

4.6. Discussion

This was the first attempt to propose a mechanistic light competition based tiller model for a more comprehensive sugarcane crop model like CANEGRO. The mechanistic model still has limitations since it excludes water stress and was calibrated and validated against data from one site, soil and harvest cycle. It has, however, introduced various new mechanistic properties and simulated tiller population and light interception with a 40% improved accuracy.

The model uses newly developed functions to model tillering and tiller senescence under light competitive conditions. Five new mechanistic crop parameters were defined. (1) The telomechron interval, which represents the minimum interval size between the emergence of consecutive tillers, was argued to be more complex than a single fixed value and could be shorter for higher order tillers. (2) A fixed ratio between tiller population at harvest and the number of primary tillers that will emerge in the consecutive ratoon enables the model to account for differences between ratoons. In conjunction with this, (3) a stool-diameter factor was introduced. This factor could be used in more than one way and also contributed to the model's effectiveness in simulating differences between consecutive ratoons. (4) A universal trend was used to simulate the relative tillering rate as a function of light interception. There are indications that this relationship could also be used to improve the simulation of stalk elongation. (5) A minimum sustainable leaf area per tiller under light competitive conditions

was found to be determined by the stool diameter and leaf area index. This parameter was used to simulate tiller senescence in a more mechanistic way.

Overall, the model represents an improvement to the CANEGRO model's tiller population component and should provide the basis for further advancement in the science of crop modelling.

Chapter 5

CONCLUSION

The first objective of the study was to initiate the review process of the CANEGRO sugarcane model. The overviews of Chapters 2 and 3 have been the most comprehensive of their kind and provides a stepping stone for more detailed future reviews. Analyses that were done on the model code retrieved valuable information that has not been formally documented before. In conjunction with the literature survey, relevant scientific publications have not only been integrated by means of reference, but a standardised set of model parameters and measurement units have been collated.

Various plant related areas where the model could be improved have been mentioned at the end of each section. The absence of a mechanistic approach in the model's calculation of population was considered to be a limiting factor when different planting and harvesting practices are simulated. The inclusion of a growth respiration component during the simulation of negative growth was questioned. Further to this, emphasis was laid on the fragmentation between biomass partitioning and the development of individual plant organs, like leaves, stalks and roots. The simulation of the effect of water stress on tillers was also suggested to form part of possible future refinements to the model.

The second objective of this study, which aimed at integrating and refining the simulation of tiller population was addressed in Chapter 4. The study has produced one of the first mechanistic sugarcane tiller population models. This model has not only indicated its ability to outperform the existing model, but also introduces opportunities to apply this type of model to new light competition related studies like optimal row spacing, high density planting and inter-cropping. Since this is one of the first proposed mechanistic tiller models, it is

anticipated that, if well calibrated, the model will not only enhance the functionality of the CANEGRO model, but could also be implemented into various other sugarcane models. The introduction of a more statistical approach has stimulated new suggestions in the way water stress, partitioning and differences between tillers of different ages could be modelled. It is anticipated that this method could be extended to many other crop properties in a stochastic way.

The mechanistic nature of the model clarifies tiller processes and leans itself towards future model refinement and expansion. The proposed model enables the simulation of consecutive ratoon crops by defining stool width dynamics and a relationship between the previous crop's mature state and the new crop's emergence phase. The processes of tillering and tiller senescence is also better understood with regard to light interception and stimulates suggestions for future research in this field.

5.1. Future work with regard to tiller modelling

The proposed tiller model is in its infancy and further research is required to make the model more applicable for the simulation of commercial sugarcane crops. To conclude, some likely fruitful studies are suggested below.

- With a more mechanistic tiller model in place, future studies can aim at calibrating parameters for different soils, sites, harvesting cycles and especially different cultivars.
- The influence of different harvesting and planting practices on bud germination should also be investigated.
- It is expected that some of the crop phases will overlap and more comprehensive recordings and analysis need to be done to resolve this question.

- Secondary tillers receiving photosynthate from parent tillers are sustainable, regardless of the levels of light competition in the crop. More research into this field will not only reveal when tillers become unsustainable, but will also address partitioning issues that can be used in other components of the CANEGRO model.
- Stalk elongation is related to light competition. The proposed model initiated some concepts of light competition and stalk elongation could be linked to these concepts.
- The telomechron interval is expected to be more complex than one fixed value used in this study. More comprehensive tillering observations are required to improve this concept since higher order tillers are expected to emerge sooner than lower order tillers.
- The implementation of a stool diameter adjustment factor indicates the necessity for further investigations into the crop's inhomogeneous hedgerow structure and to adjust light interception accordingly.
- The simulation of water stress has not been included into the proposed model. Since water stress is a very active and frequently observed phenomena in commercial sugarcane crops, it should be regarded as one of the more important limitation to the proposed tiller model.

References

Allen, R.G., Jensen, M.E, Wright, J.L., Burman, R.D., 1989, Operational estimates of reference evapotranspiration., *Agron Journal* **81**: p650-662.

Anderson, E.L., 1987, Crop root growth and distribution as influenced by tillage and nitrogen fertilization. *Agron Journal* **79**: p544-549.

ASCE, 1990, Evapotranspiration and Irrigation Water Requirements., *American Society of Civil Engineers*, New York, ISBN 0-87262-763-2, 331pp.

Barber, S.A., 1971, Effect of tillage practice on corn (*Zea Mays* L.) root distribution and morphology. *Agron Journal* **63**: p724-726.

Bouman, B.A.M., Kasteren, H.W.J., Uenk, D., 1992, Standard relations to estimate ground cover and *LAI* of agricultural crops from reflectance measurements., *Eur. J. Agron* **4**:(4) p149-162.

Cochran, B.J., Richaud, R., 1980, Mechanization of high population sugarcane in Louisiana., *Proc. I.S.S.C.T.* **17**: p1069-1077.

Coleman, R.E., 1968, Physiology of flowering in sugarcane., *Proc. I.S.S.C.T.* **13**: p192-1000.

Crop Science Society of America (CSSA), 1991, Modeling crop Photosynthesis – from biochemistry to canopy. *Ed.* Boote, K.J., Loomis, R.S., *Am Soc of Agron, Inc.*, Madison, USA, ISBN 0-89118-533-X, 140pp.

De Jager, J.M., van Zyl, W.H., 1989, Atmospheric evaporative demand and evaporation coefficient concepts., *Water SA*, ISBN 0378-4738, **15**: p103-110.

Essenwanger, O., 1976, Applied statistics in atmospheric science. Part A. Frequencies and curve fitting., *Elsevier scientific publishing comp.*, Amsterdam, ISBN 0-444-41327-8, 412pp.

Glover, J., 1972, Practical theoretical assessments of sugarcane yield potential in Natal., *Proc S Afr Sug Technol Ass* **46**: p138-141.

Gosnell, J.M., 1971, Some effects of a water-table level on the growth of sugarcane., *Proc S Afr Sug Technol Ass* **14**: p841-849.

Gray, P., 1967, The dictionary of the biological sciences., *Reinhold publishing corporation*, New York, 602pp.

Hesketh, J.D., Baker, D.N., Duncan, W.G., 1971, Simulation of growth and yield in cotton: respiration and carbon balance. *Crop Sci* **11**: p394-398.

Hillel, D., 1982, Introduction to Soil Physics., *Academic Press*, New York, 364pp.

Inman-Bamber, N.G., 1985, Factors affecting the performance of varieties released recently in the South African sugar industry., *Proc S Afr Sug Technol Ass* **59:** p5-9.

Inman-Bamber, N.G., 1986, The reaction of sugarcane to water stress., Ph.D. thesis, *University of the Orange Free State*, Bloemfontein.

Inman-Bamer, N.G., Thompson, G.D., 1989, Models of dry matter accumulation by sugarcane. *Proc S Afr Sug Technol Ass* **63**: p212-216.

Inman-Bamber, N.G., 1991, A growth model for sugar-cane based on a simple carbon balance and the CERES-Maize water balance., *S. Afr. J. Plant Soil* **8**(2): p93-99.

Inman-Bamber, N.G., Culverwell, T.L., McGlinchey, M.G., 1993, Predicting yield responses to irrigation of sugarcane from a growth model and field records., *Proc S Afr Sug Technol Ass* **67**: p66-72.

Inman-Bamber, N.G., 1994a, Effect of age and season on components of yield of sugarcane in South Africa., *Proc. S Afr Sug Technol Ass* **68**: p23-27.

Inman-Bamber, N.G., 1994b, Temperature and seasonal effects on canopy development and light interception of sugarcane., *Field Crops Research* **36**: p41-51.

Inman-Bamber, N.G., 1995b, Climate and water as constraints to production in the South African sugar industry., *Proc S Afr Sug Technol Ass* **69**: p55-59.

Inman-Bamber, N.G., Kiker, G., 1997, CANEGRO 3.10. DSSAT version 3.1 1998 distribution software. *IBSNAT*, University of Hawaii, Honolulu, Hawaii, USA.

Jackson, R.D., Idso, S.B., Reginato, R.J., 1976, Calculation of evaporation rates during the transition from energy-limiting to soil-limiting phases using albedo data., *Water Resour Res* **12**: p23-26.

Jones, C.A., Kiniry, J.R., 1986, CERES-Maize: A simulation model of maize growth and development., *Texas A&M university press*, College Station, USA, ISBN 0-89096-269-3, 194 pp.

Kanwar, R.S., Sharma, K.K., 1974, Effect of inter-row spacing on tiller mortality, stalk population and yield of sugarcane., *Proc ISSCT* **15**: p751-755.

Keating, B.A., Robertson, M.J., Muchow, R.C., Huth, N.I., 1999, Modelling sugarcane production systems I. Development and performance of the sugarcane module., *Field crops research* **3767**: p1-19.

Leslie, G.W., 1997, Research strategies for the use of insecticides to control sugarcane pests in South Africa., *Proc. S Afr Sug Technol Ass* **71**: p91-93.

Lorber, M.N., Fluck, R.C., Mishoe, J.W., 1984, A method for analysis of sugarcane (*Saccharum sp*) biomass production systems., *Transactions of the Am Soc Agric Engr* **27**: p146-158.

Mathews, J.H., 1987, Numerical methods for computer science, engineering, and mathematics., *Prentice-Hall International, Inc.*, London, ISBN 0-13-626565-0, 507pp.

McGlinchey, M.G., Inman-Bamber, N.G., Culverwell, T.L. and Els, M., 1995, An irrigation scheduling method based on a crop model and an automatic weather station., *Proc S Afr Sug Technol Ass* **69**: p69-73.

McGlinchey, M.G., Inman-Bamber, N.G., 1996, Predicting sugarcane water use with the Penman-Monteith equation., Proc. of Evapotranspiration and irrigation scheduling, *American Society of Agricultural Engineers*, p592-597.

Meyer, B.S., Anderson, D.B., Böhning, R.H., 1960, Introduction to Plant Physiology., *D. van Nostrand Comp. Ltd.*, London, UK, 541pp.

Meyer, J.H., Wood, R.A., 1994, Nitrogen management of sugar cane in South Africa., *Proc Aus Soc Sug Technol* **16**: p93-97.

Mishoe, Jones, Gasco, 1979, Harvesting scheduling of sugarcane for optimum biomass production. *Transactions of the Am Soc Agric Engr* **22**: p1299-1304.

Monteith, J.L., 1965, Evaporation and environment. In: The State and Movement of Water in Living Organisms. *Proc of 18th Symposium of the Society of Experimental Biology*, Swansea, Cambridge University Press. p205-233.

Muchow, R.C., Coates, D.B., Wilson, G.L., Foale, M.A., 1982, Growth and productivity of *Sorghum bicolor* (L. Moench) in Northern Australia, 1. Plant density and arrangement effects on light interception and distribution and grain yield, in hybrid Texas 610SR in low and medium latitudes. *Aust. J. Agric. Res.* **33**: p773-784.

O'Leary, G.J., Connor, D.J., 1996, A Simulation model of the wheat crop in response to water and nitrogen supply: I. Model construction., *Agricultural Systems* **52**: p1-29.

Penman, H.L., 1948, Natural evaporation from open water, bare soil and grass. *Proc Royal Soc* **A193**: p120-145.

Philip, J.R., 1959, Evaporation and moisture and heat fields in the soil. *Journal of Meteorology* **14**: p354-366.

Priestley, C.H.B., Taylor, R.J., 1972, On the assessment of surface heat flux and evaporation using large scale parameters., *Mon Weath Rev* **100**: p81-92.

Rending, V.V., Taylor, H.M., 1989, Principles of soil-plant interrelationships., *McGraw-Hill*, New York, ISBN 0-07-051879-3.

Rice, J.A., 1995, Mathematical statistics and data analysis., 2nd Edition, *International Thompson Publishing, Wadsworth Inc.*, Belmont, California, ISBN 0-534-20934-3, 602pp.

Ritchie, J.T., Burnett, E., 1971, Dryland evaporative flux in a subhumid climate: II. Plant influences., *Agron Journal* **63**: p56-62.

Ritchie, J.T., Godwin, D.G., Singh, U., 1989, Soil and weather inputs for the IBSNAT crop models., *Proc of the IBSNAT symposium: Decision Support System of Agrotechnology Transfer*, Las Vegas, Part I: Symposium procedings Dept. of Agr. and Soil Sci. University of Hawaii, Honolulu, Hawaii.

Robertson, M.J., Fukai, S., Hammer, G.L., Ludlow, M.M., 1993, Modelling root growth of grain sorghum using the CERES approach., *Field Crops Research* **33**: p113-130.

Robertson, M.J., Donaldson, R.A., 1998, Changes in the components of cane and sucrose yield response to drying-off of sugarcane before harvest., *Field crops research* **55**: p201-208.

Rostron, H., 1972, Some effects of environment, age and growth-regulating compounds on the growth, yield and quality of sugarcane in southern Africa. Ph.D. thesis, *University of Natal*, Pietermaritzburg.

Rostron, H., 1974, Radiant energy interception, root growth, dry matter production and the apparent yield potential of two sugarcane varieties., *Proc S Afr Sug Technol Ass* **15**: p1001-1010.

Sanchez, D.A., Allen, R.C., Kyner, W.T., 1988, Differential equations, 2nd Edition, *Addison-Wesley Publishing comp.*, Reading, Massachusetts, ISBN 0-201-15407-2, 760pp.

Schmidt, E.J., Schulze, R.E., 1987, Flood volume and peak discharge from small catchments in Southern Africa, based on the SCS technique., *Agricultural Catchments Research Unit*, Report No. **24**, Pietermaritzburg, SA, 164pp.

Schulze, R.E., Schmidt, E.J., Smithers, J.C., 1992, SCS-SA user manual., *Agricultural Catchments Research Unit*, Report No. **40**, Pietermaritzburg, SA, 78pp.

Serway, R.A., 1986, Physics for scientists & engineers with modern Physics., 2nd Edition, *Saunders College Publishing*, Rinehart, USA, ISBN 0-03-004854-0, 1108pp.

Singels, A., Kennedy, A.J., Bezuidenhout, C.N., 1998, IRRICANE: A simple computerised irrigation scheduling method for sugarcane., *Proc S Afr Sug Technol Ass* **72**: p117-122.

Singels, A., Bezuidenhout, C.N., 1999, The relationship between ENSO and rainfall and yield in the South African sugar industry., *S. Afr. J. Plant Soil* **16**(2): p96-101.

Smith, M., 1992, Expert consultation on revision of FAO methodologies for crop water requirements., *United Nations*, Rome, 60pp.

Spitters, C.J.T., Toussaint, H.A.J.M. and Goudriaan, J., 1986, Separating the diffuse and direct component of global radiation and its implications for modeling canopy photosynthesis. Part 1. Components of incoming radiation., *Agric For Meteorol* **38**: p217-229.

Thompson, G.D., 1976, Water use by sugarcane., *S Afr Sugar J.* **60**: 593-600, 627-635

Thompson, G.D., 1978, The production of biomass by sugarcane., *Proc S Afr Sug Technol Ass* **52**: p180-187.

Thompson, G.D., 1986, Agrometeorological and crop measurements in a field of irrigated sugarcane. Mount Edgecombe Research Report No. 5. (Publ) *South African Sugar Association Experiment Station*, Mt. Edgecombe, KwaZulu Natal, SA. 244pp.

Thornley, J.H.M., 1976, Mathematical models in plant physiology., *Academic Press Inc.*, London, ISBN 0-12-690550-9, 318pp.

Van Antwerpen, R., Meyer, J.H., Inman-Bamber, N.G., 1993, Cane root development and crop modelling., *Proc S Afr Sug Technol Ass* **67**: p73-77.

Van Antwerpen, R., 1998, Modelling root growth and water uptake of sugarcane cultivar NCo 376., Ph.D. thesis, *University of the Orange Free State*, Bloemfontein. 133pp.

Van Antwerpen, R., 1999, Sugarcane root growth and relationships to above ground biomass., *Proc S Afr Sug Technol Ass* **73** (in press).

Van Dillewijn, C., 1952, *Botany of sugarcane*. Waltham., Mass., USA, 371pp.

Wang, J.Y., 1967, Acricultural meteorology., *Agricultural Weather Information Service*, San Jose, California, 693pp.

Way, M.J., 1995, Developmental biology of the immature stages of *Eldana saccharina* Walker (Lepidoptera: pyralidae)., *Proc S Afr Sug Technol Ass* **69**: p83-86.

Appendix A

Equations for leaf dimension properties for different cultivars as extracted from the CANEGRO model code. Dimensions are expressed as a function of the sequential leaf number (j).

Table A.1. Leaf blade length (l) and width (w) restrictions for different cultivars.

Cultivar	l_j (mm)	w_j (mm)
NCo376	$\begin{cases} 218 + 122j - 3.76j^2 & \lvert j \le 23 \\ 1000 & \lvert j > 23 \end{cases}$	$\begin{cases} 7.75 + 2.243j - 0.0345j^2 & \lvert j \le 49 \\ 35 & \lvert j > 49 \end{cases}$
N12	$\begin{cases} 218 + 122j - 3.76j^2 & \lvert j \le 18 \\ 1200 & \lvert j > 18 \end{cases}$	$\begin{cases} 7.75 + 2.243j - 0.0345j^2 & \lvert j \le 44 \\ 40 & \lvert j > 44 \end{cases}$
N14	$\begin{cases} 130 + 92j & \lvert j \le 14 \\ 1500 & \lvert j > 14 \end{cases}$	$7.75 + 2.243j - 0.0345j^2$
R570	$\begin{cases} -55.9 + 225.58j - 10.58j^2 + 0.1623j^3 & \lvert j \le 20 \\ 1530 & \lvert j > 20 \end{cases}$	$\begin{cases} 14.7 + 2.418j & \lvert j \le 20 \\ 63 & \lvert j > 20 \end{cases}$

Table A.2. The maximum potential leaf area (A_{max}) for different leaves and different cultivars.

Cultivar	$A_{max(j)}$ (mm^2)
NCo376	$\begin{cases} -208 + 272j & \lvert j \le 15 \\ 3872 & \lvert j > 15 \end{cases}$
N12	$-90 + 317j$
N14	$\begin{cases} 7.75 + 2.243j - 0.0345j^2 & \lvert j \le 15 \\ 4000 & \lvert j > 15 \end{cases}$
R570	$\begin{cases} -110 + 357j & \lvert j \le 20 \\ 7140 & \lvert j > 20 \end{cases}$

Appendix B

The method that was used to derive likelihood values for the p and q parameters of the beta distribution function.

Rice (1995: 594) noted that the mean and variance of a beta distribution ranging between 0 and 1 can respectively be derived from eqs. 1 and 2 below.

$$\bar{x} = \frac{p}{p+q} \qquad (1)$$

$$\therefore q = \frac{p}{\bar{x}} - p \qquad (1.b)$$

and

$$\sigma^2 = \frac{pq}{(p+q)^2(p+q+1)} \qquad (2)$$

$$= \frac{p}{p+q} \times \frac{p}{p+q} \times \frac{q}{p(p+q+1)}$$

$$= \frac{\bar{x}^2 q}{p(p+q+1)}$$

$$\therefore \sigma^2 p^2 + \sigma^2 pq + \sigma^2 p - \bar{x}^2 q = 0 \qquad (2.b)$$

Now substitute 1.b in 2.b:

$$\sigma^2 p^2 + \frac{\sigma^2 p^2}{\bar{x}} - \sigma^2 p^2 + \sigma^2 p - p\bar{x} + p\bar{x}^2 = 0$$

$$\therefore \sigma^2 p + \sigma^2 \bar{x} - \bar{x}^2 + \bar{x}^3 = 0$$

$$\therefore p = \frac{-(\sigma^2 \bar{x} - \bar{x}^2 + \bar{x}^3)}{\sigma^2}$$

For a beta distribution that ranges from LA_{min} to LA_{max}, it can be shown that

$$\overline{LA} = \bar{x}(LA_{max} - LA_{min}) + LA_{min}$$

and

$$\sigma_{LA}^2 = \sigma^2(1.1LA_{\max} - 0.9LA_{\min})^2$$